Hungarian Space Office

SZENT ISTVÁN UNIVERSITY

esa

→ 7th ADVANCED TRAINING COURSE ON LAND REMOTE SENSING

4–9 September 2017 | Szent István University | Gödöllő, Hungary

INTRODUCTION TO THERMAL REMOTE SENSING

Professor Constantinos Cartalis
Department of Environmental Physics
Remote Sensing and Image Processing Research Unit
National and Kapodistrian University of Athens
ckartali@phys.uoa.gr

Learning Objectives

What is thermal remote sensing?

Which are the laws describing thermal remote sensing?

What is the difference between kinetic temperature and radiant temperature?

What is emissivity and why is it relevant to thermal remote sensing?

How is land surface temperature influenced by the thermal properties of materials?

How to interpret thermal images?

How is land surface temperature estimated?

Which applications can be supported?

The three basic ways in which energy can be transferred:

• *Conduction* occurs when one body (molecule or atom) transfers its kinetic energy to another by colliding with it. This is how a pan is heated on a stove.

• In *convection*, the kinetic energy of bodies is transferred from one place to another by physically moving the bodies. An example is the convectional heating of air in the atmosphere in the early afternoon.

• The transfer of energy by ***electromagnetic radiation*** is of primary interest to remote sensing because it is the only form of energy transfer that can take place in a vacuum such as the region between the Sun and the Earth.

Thermal capacity (c) is the ability of a material to store heat. It is measured as the number of calories required to raise a gram of material (e.g. water) 1 ˚C (cal g-1 ˚C-1). Water has the highest thermal capacity (1.00). It stores heat very well relative to all the other materials.

• *Thermal conductivity* (K) is the rate that heat will pass through a material and is measured as the number of calories that will pass through a 1-cm cube of material in 1 second when two opposite faces are maintained at 1 ˚C difference in temperature (cal cm^{-1} sec^{-1} ˚C). The conductivity of a material is variable due to soil moisture and particle size. Many rocks and soils are extremely poor conductors of heat.

Thermal inertia (P) is a measurement of the thermal response of a material to temperature changes and is measured in calories per square centimeter per second square root per degree Celsius (cal cm^{-2} sec $^{-1/2}$ °C^{-1}).

Thermal inertia is computed using the equation:

$$P = (K \times p \times c)^{1/2}$$

where *K* is thermal conductivity, *p* is density (g cm^{-3}), and *c* is thermal capacity. Density is the most important property in this equation because thermal inertia generally increases linearly with increasing material density.

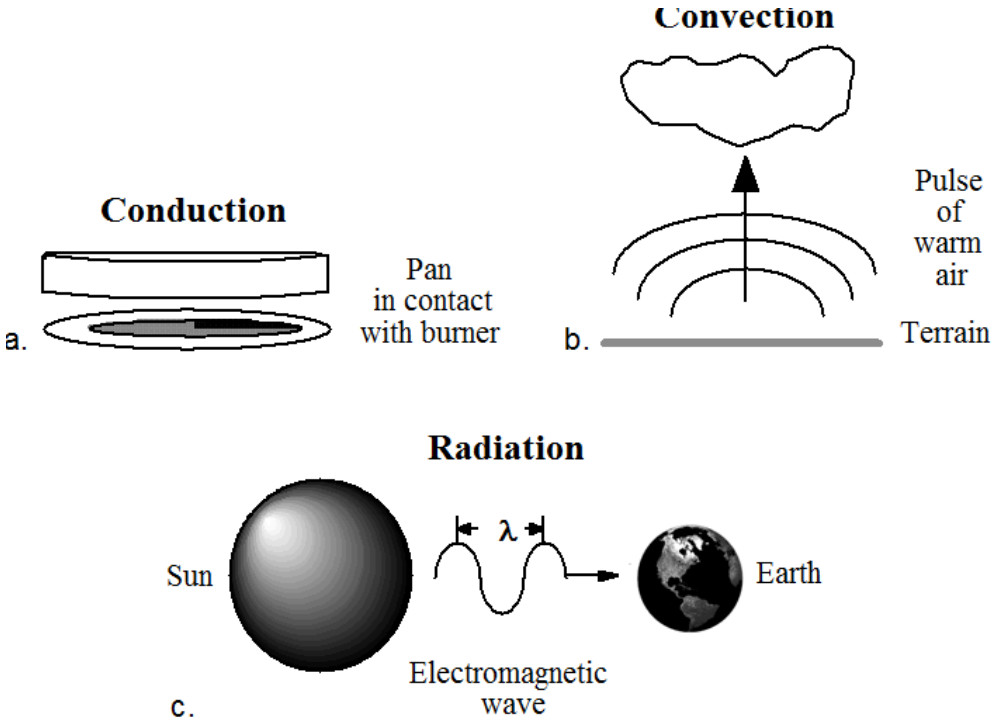
Conduction
a.
Pan
in contact
with burner
Convection
Pulse
of
warm
air
b.
Terrain
Radiation
Sun
λ
Earth
Electromagnetic
wave
c.

Optical vs thermal remote sensing

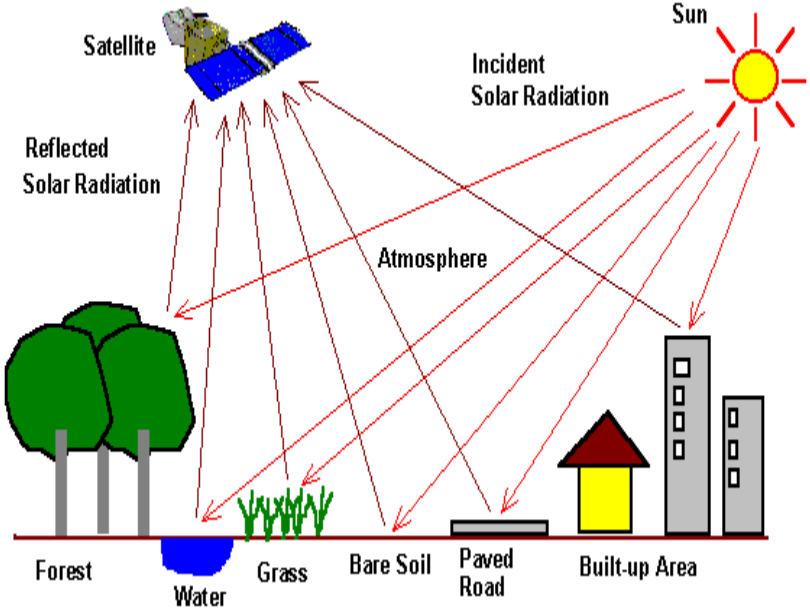

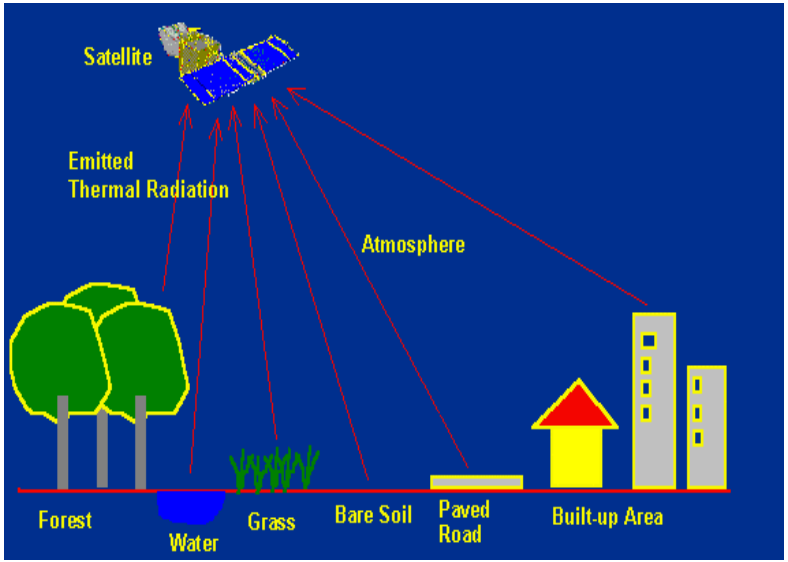


OK

- In remote sensing the IR band is usually divided into two components that are based on basic property differences;
  - Reflected IR band : The reflected IR band represents reflected solar radiation which behaves like visible light. Its wavelength span is from 0.7 to about 3 micrometers.
  - Emitted/Thermal IR band : The dominant type of energy in the thermal IR band is heat energy, which is continuously emitted by the atmosphere and all objects on the earth' s surface. Its wavelength span is from about 3 micrometers to 4 micrometers.

Two components

Reflected IR band: from 0.7 μm to about 3 μm

Emitted/Thermal IR band: heat energy is the dominant source as emitted from the earth and the atmosphere. The spectral interval spans from 3 μm to roughly 14 μm.

In particular thermal mapping of the earth's surface is possible in the spectral intervals from 3-5 μm and 8-14 μm.

Introductory points - 2

The reason we can use remote sensing devices to detect infrared energy in these regions is because the atmosphere allows a portion of the infrared energy to be transmitted from the terrain to the detectors.

Regions that pass energy are called ***atmospheric windows***.

Regions that absorb most of the infrared energy are called ***absorption bands***. Water vapor (H_2O), carbon dioxide (CO_2), and ozone (O_3) are responsible for most of the absorption.

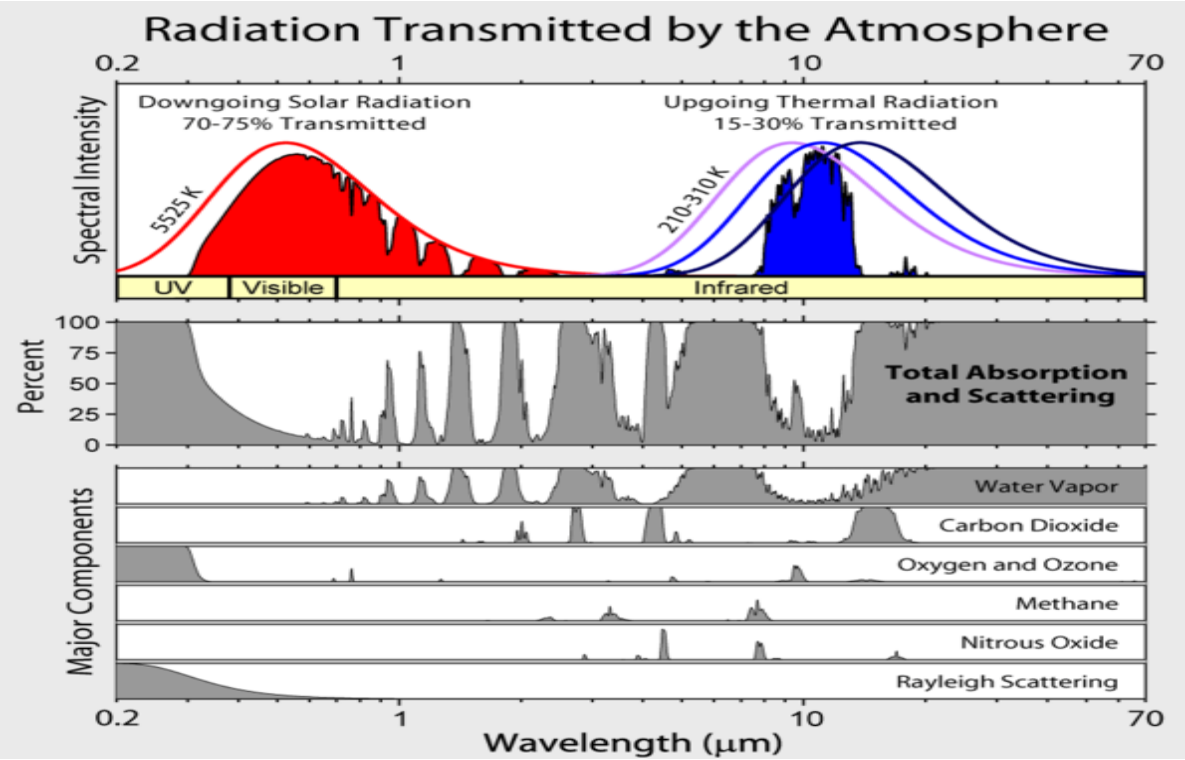
Radiation Transmitted by the Atmosphere
0.2
1
10
70
Spectral Intensity
Downgoing Solar Radiation
70-75% Transmitted
Upgoing Thermal Radiation
15-30% Transmitted
5525 K
210-310 K
UV
Visible
Infrared
Percent
100
75
50
25
0
Total Absorption and Scattering
Major Components
Water Vapor
Carbon Dioxide
Oxygen and Ozone
Methane
Nitrous Oxide
Rayleigh Scattering
0.2
1
10
70
Wavelength (μm)

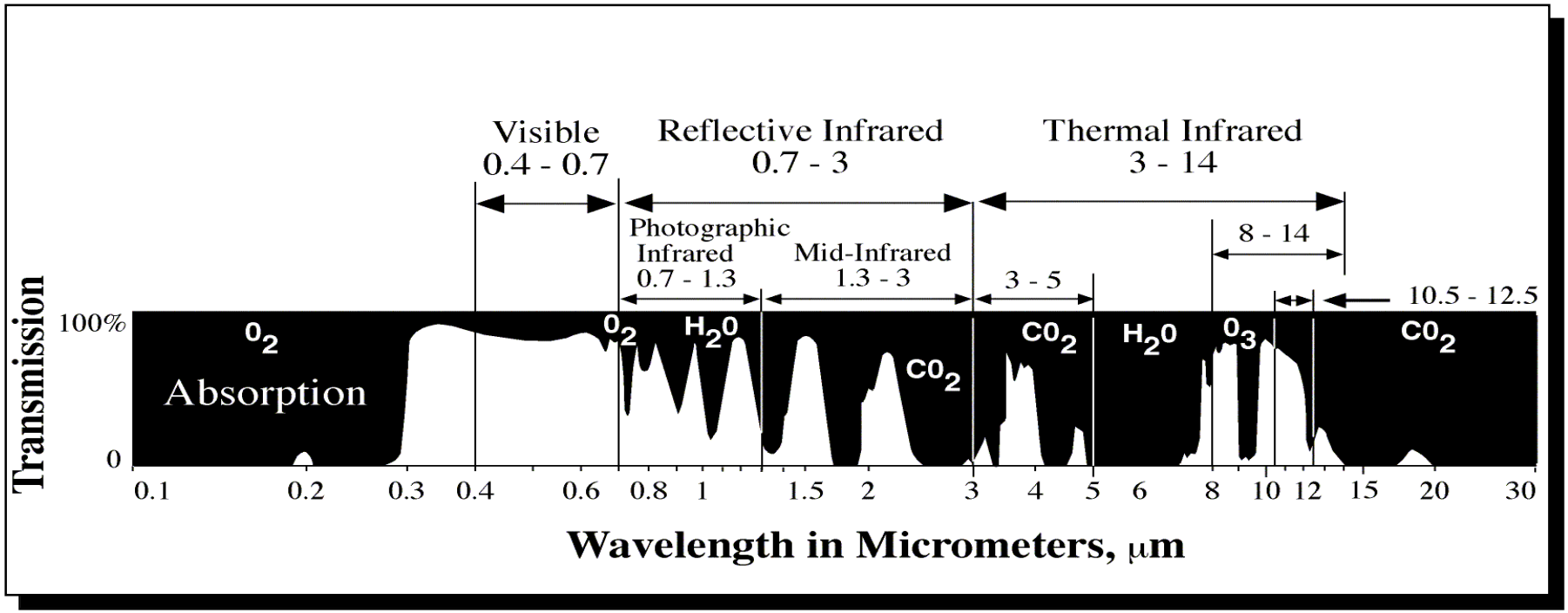
Visible
0.4 - 0.7
Reflective Infrared
0.7 - 3
Thermal Infrared
3 - 14
Photographic
Infrared
0.7 - 1.3
Mid-Infrared
1.3 - 3
3 - 5
8 - 14
10.5 - 12.5
Transmission
100%
0
O_2
Absorption
O_2
H_2O
CO_2
CO_2
H_2O
O_3
CO_2
0.1
0.2
0.3
0.4
0.6
0.8
1
1.5
2
3
4
5
6
8
10
12
15
20
30
Wavelength in Micrometers, μm

Introductory points - 3

An object's **internal kinetic heat** is converted to **radiant energy** (often called external or apparent energy).

The electromagnetic radiation exiting an object is called ***radiant flux*** and is measured in watts. The concentration of the amount of radiant flux exiting (emitted from) an object relates to its radiant temperature (T_{rad}).

• There is usually a high positive correlation between the true kinetic temperature of an object (T_{kin}) and the amount of radiant flux radiated from the object (T_{rad}). Therefore, we can utilize radiometers placed some distance from the object to measure its radiant temperature which correlates well with the object's true kinetic temperature. ***This is the basis of thermal infrared remote sensing.***

Yet, the correlation (and the resulting relationship) is not perfect, with the remote measurement of the radiant temperature always being **slightly less** than the true kinetic temperature of the object.

This is due to a thermal property called **emissivity.**

Introductory points - 4

A ***blackbody*** is a theoretical construct that absorbs all the radiant energy striking it and radiates energy at the maximum possible rate per unit area at each wavelength for any given temperature.

• No objects in nature are true blackbodies, however, we may think of the Sun as approximating a 6,000 ˚K blackbody and the Earth as a 300 ˚K blackbody.

If we pointed a sensor at a blackbody we would be able to record quantitative information about the total amount of radiant energy in specific wavelengths exiting the object and the dominant wavelength of the object. In order to do this, we utilize some important physical laws: **the Planck law, the Stefan-Boltzmann law and Wein's displacement law.**

Important point

The real world is not composed of radiating blackbodies.

Rather it is composed of selectively radiating bodies such as rocks, soil, and water that emit only a fraction of the energy emitted from a blackbody at the same temperature.

Emissivity, ε, is the ratio between the radiant flux exiting a real-world selective radiating body (F_r) and a blackbody at the same temperature (F_b).

All selectively radiating bodies have emissivities ranging from 0 to <1 that fluctuate depending upon the wavelengths of energy being considered.

A graybody outputs a constant emissivity that is less than one at all wavelengths.

Some materials like distilled water have emissivities close to one (0.99) over the wavelength interval from 8 - 14 μm.

Others such as polished aluminum (0.08) and stainless steel (0.16) have very low emissivities.

Radiation of real Materials

Emissivity depends on wavelength, surface temperature, and some physical properties of the surface, e.g. water content, or density.

Material	Average Emissivity over 8-14 µm
Clear water	0.98 - 0.99
Healthy green vegetation	0.96 - 0.99
Dry vegetation	0.88 - 0.94
Asphaltic concrete	0.94 - 0.97
Basaltic rock	0.92 - 0.96
Granitic rock	0.83 - 0.87
Dry mineral soil	0.92 - 0.96
Polished metals	**0.06 - 0.21**

Source: Lillesand et al. (2008)

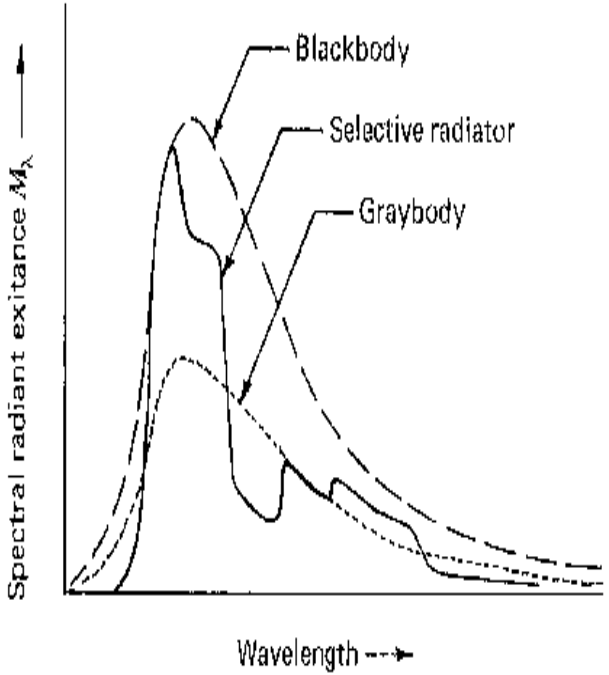

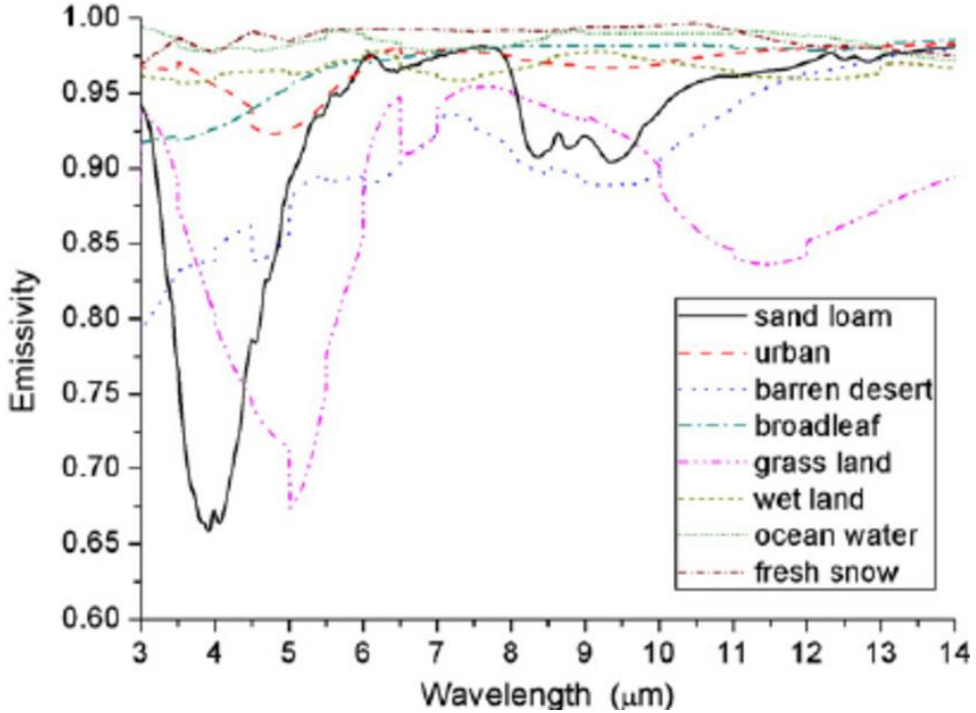

Source: Tang and Li, 2008
Remote Sensing of Environment

Planck blackbody equation:

describes the EM radiation emitted from a blackbody at a certain wavelength as a function of its absolute temperature

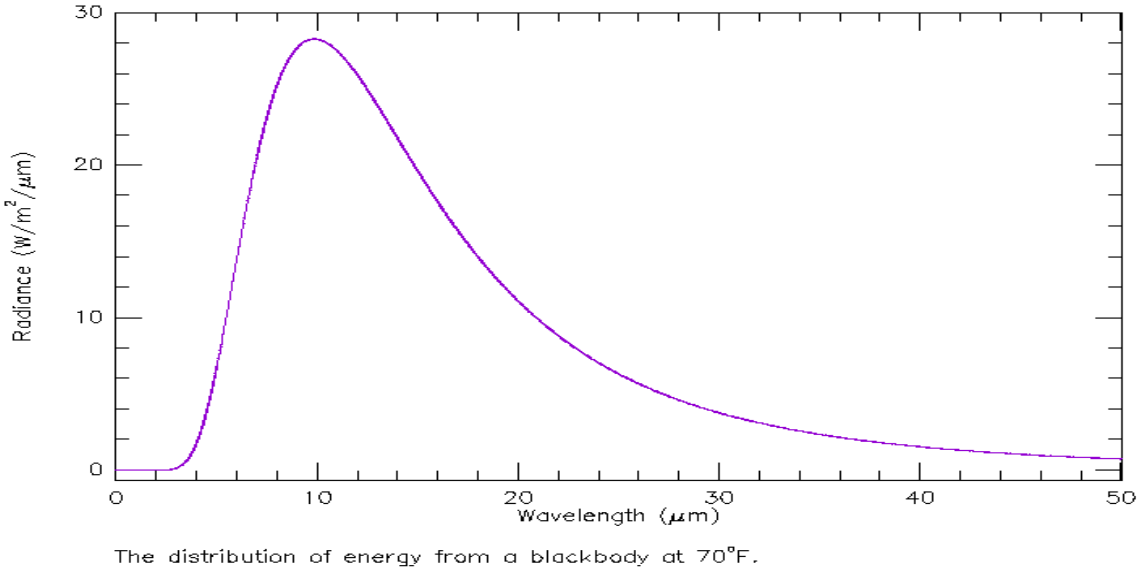

The distribution of energy from a blackbody at 70°F.

$$B(\lambda,T)=\frac{2\pi hc^2}{\lambda^5(e^{hc/(\lambda kT)}-1)}$$

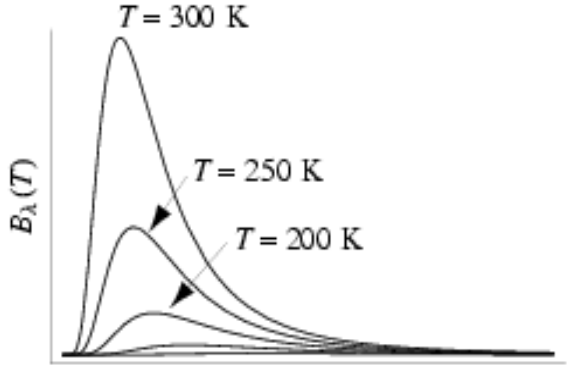

Planck equation for blackbody radiance

$$B_\lambda = \frac{2\pi hc^2}{\lambda^5 (e^{\frac{hc}{k\lambda T}} - 1)}$$

→ radiance temperature $T_R = T_B$
(brightness temperature)

$$T_B = \frac{K_2}{\ln\left(\frac{K_1}{B_\lambda} + 1\right)}$$

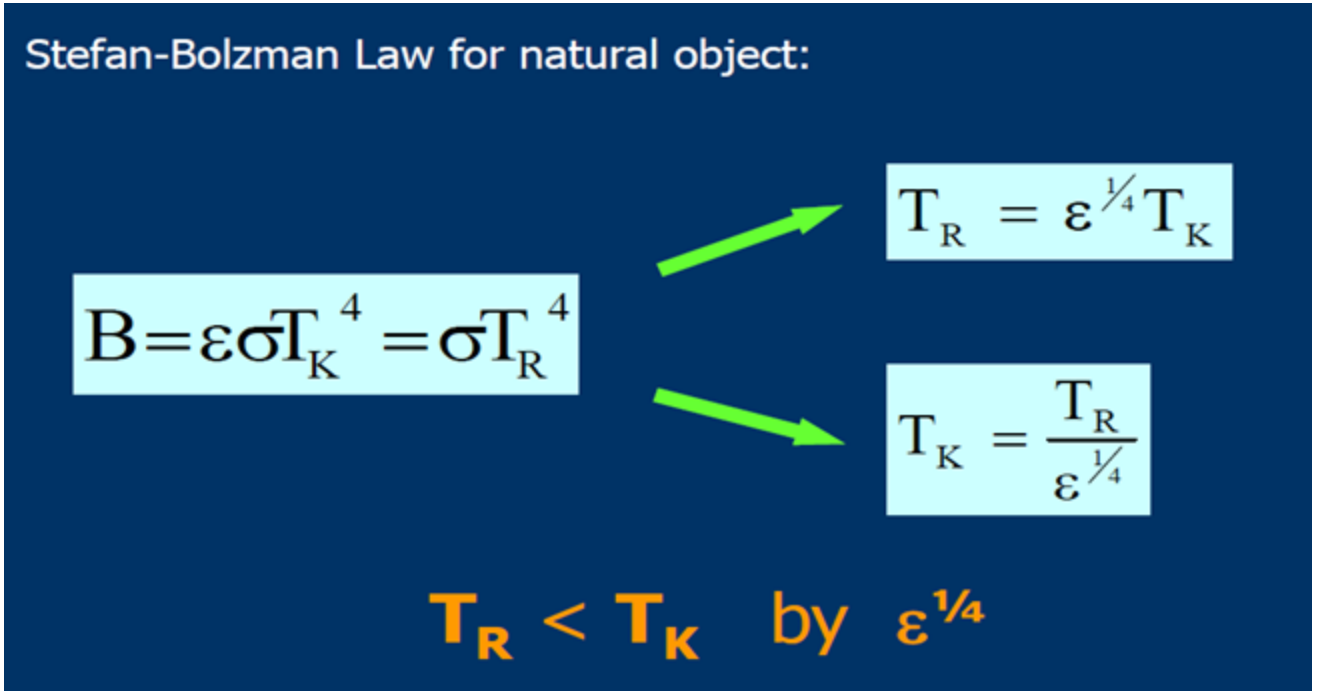

T_K the kinetic temperature

Wien's displacement Law

The relationship between the true temperature of a blackbody (*T*) in degrees Kelvin and its peak spectral exitance or dominant wavelength (λ_{max}) is described by Wein's displacement law:

$$\lambda_{max} = \frac{k}{T} = \frac{2898\ \mu m\ ^{\circ}K}{T}$$

where *k* is a constant equaling 2898 μm $^{\circ}$K.

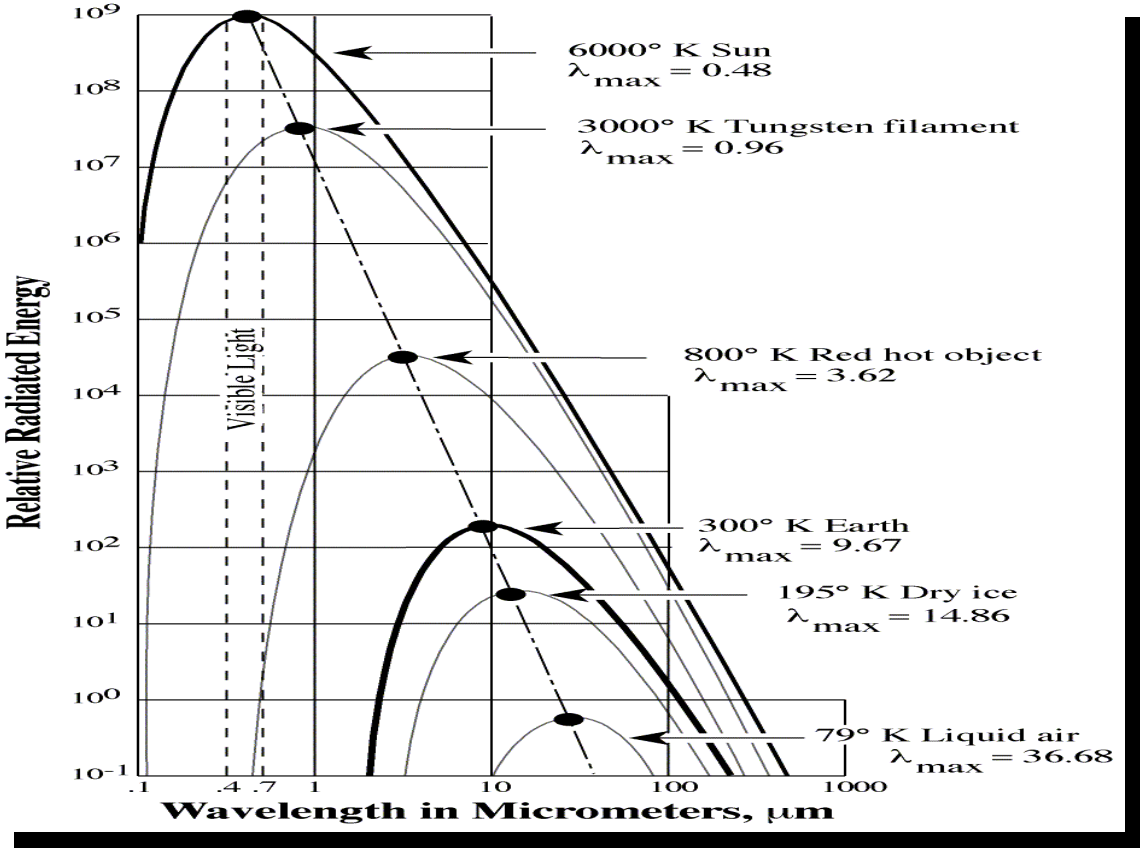
Relative Radiated Energy
10^9
10^8
10^7
10^6
10^5
10^4
10^3
10^2
10^1
10^0
10^{-1}
Visible Light
6000° K Sun
$\lambda_{max} = 0.48$
3000° K Tungsten filament
$\lambda_{max} = 0.96$
800° K Red hot object
$\lambda_{max} = 3.62$
300° K Earth
$\lambda_{max} = 9.67$
195° K Dry ice
$\lambda_{max} = 14.86$
79° K Liquid air
$\lambda_{max} = 36.68$
.1
.4
.7
1
10
100
1000
Wavelength in Micrometers, μm

The **dominant** wavelength

The dominant wavelength provides information about which part of the thermal spectrum we might want to sense in.

For example, if we are looking for **800 ˚K forest fires** that have a dominant wavelength of approximately **3.62 µm** then the most appropriate remote sensing system might be a **3-5 µm** thermal infrared detector.

• If we are interested in **soil, water, and rock with ambient temperatures on the earth's surface of 300 ˚K** and a dominant wavelength of **9.66 µm**, then a thermal infrared detector operating in the **8 - 14 µm** region might be most appropriate.

Remember that the terrain intercepts incident (incoming) radiant flux.

This incident energy interacts with terrain materials.

The general equation for the interaction of **spectral** radiant flux with the terrain is:

Spectral radiant flux = the amount of radiant flux reflected from the surface + the amount of radiant flux absorbed by the surface + the amount of radiant flux transmitted through the surface.

Interaction of radiation with terrain elements

$$1 = r_\lambda + \alpha_\lambda + \tau_\lambda$$

where r_λ is spectral hemispherical reflectance by the terrain,

α_λ is spectral hemispherical absorptance, and

τ_λ is spectral hemispherical transmittance

Kirchhoff's radiation law

According to Kirchoff's radiation law for a blackbody: $\alpha_\lambda = \varepsilon_\lambda$

Thus $1 = r_\lambda + \alpha_\lambda + \tau_\lambda$ can be written as $1 = r_\lambda + \varepsilon_\lambda + \tau_\lambda$

But most real-world materials are usually opaque to thermal radiation meaning that no radiant flux exits from the other side of the terrain element. Therefore, we may assume transmittance, $\tau_\lambda = 0$

Thus: $1 = r_\lambda + \varepsilon_\lambda$

which implies that the higher an object's reflectance in the thermal infrared region, the lower the emissivity and vice versa.

For example, water absorbs almost all incident energy and reflects very little. Therefore, water is a very good emitter and has a high emissivity close to 1.

Conversely, a sheet metal roof reflects most of the incident energy, absorbs very little, yielding an emissivity much less than 1. Therefore, metal objects such as cars, aircraft, and metal roofs almost always look very cold (dark) on thermal infrared imagery.

But things are more complicated

Radiative Transfer Model (RTM)

Based on a radiative transfer equation the path of the radiation through the atmosphere can be simulated by:

$$L(\lambda) = \varepsilon(\lambda) L_B(\lambda, T) \tau(\lambda) + L_u(\lambda) + \frac{(1-\varepsilon(\lambda)) L_d(\lambda) \tau(\lambda)}{\pi}$$

at-satellite radiance	emitted surface radiance	upwelling radiance	downwelling radiance reflected at the surface

RTM (e.g. MODTRAN) is used to solve this equation by **modeling the atmospheric conditions during image acquisition**. Highly variable parameters (aerosol and water vapor content) have to be estimated carefully if no in-situ data are available. In the thermal IR region the atmospheric **water vapor** is the dominating parameter.

Scattering processes are negligible (scattering is inversely proportional to λ^4)

Source: Kuenzer, 2015

Important note for thermal analysis

Two materials on the ground could have **the same true kinetic temperature but have different apparent temperatures** when sensed by a thermal radiometer simply because their emissivities are different.

The emissivity of an object may be influenced by a number factors, including:

• color - darker colored objects are usually better absorbers and emitters (i.e. they have a higher emissivity) than lighter colored objects which tend to reflect more of the incident energy.

• surface roughness - the greater the surface roughness of an object relative to the size of the incident wavelength, the greater the surface area of the object and potential for absorption and re-emission of energy.

• moisture content - the more moisture an object contains, the greater its ability to absorb energy and become a good emitter. Wet soil particles have a high emissivity similar to water.

• compaction - the degree of soil compaction can effect emissivity.

• field-of-view/resolution - the emissivity of a single leaf measured with a very high resolution thermal radiometer will have a different emissivity than an entire tree crown viewed using a coarse spatial resolution radiometer.

• wavelength - the emissivity of an object is generally considered to be wavelength dependent. It may be constant in one spectral interval, but varying in another.

• viewing angle - the emissivity of an object can vary with sensor viewing angle.

Speaking about resolution

There is an inverse relationship between having high spatial resolution and high radiometric resolution when collecting thermal infrared data.

The larger the radiometer instantaneous-field-of-view, the longer the dwell time that an individual detector can view the terrain within the IFOV during a single sweep of the mirror. Thus a larger IFOV provides good radiometric resolution which is the ability to discriminate between very small differences in radiant energy exiting the terrain element (also provides good signal to noise ratio).

At the same time, the larger the IFOV, the poorer the ability to resolve fine spatial detail.

Temporal to spatial resolution

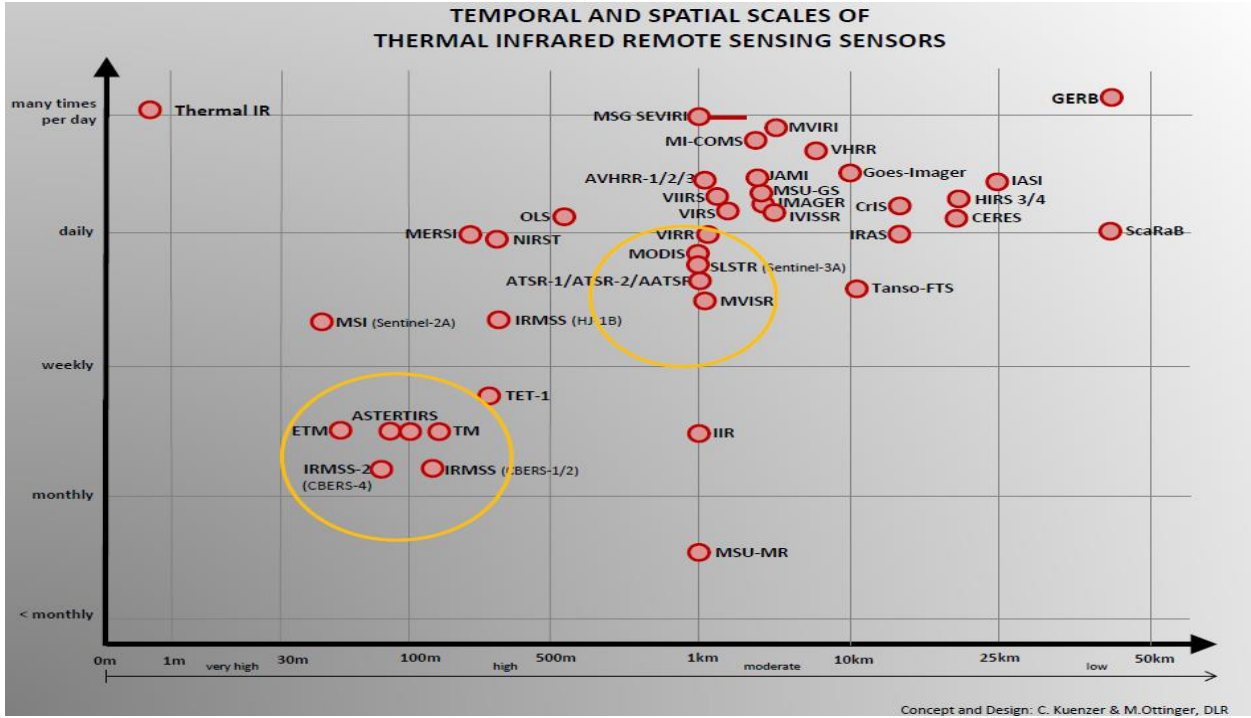

Ground area sensed

The diameter of the circular ground area viewed by the sensor, *D*, is a function of the instantaneous-field-of-view, φ, of the scanner measured in milliradians (mrad) and the altitude of the scanner above ground level, *H*, where:

$$D = H \times \varphi$$

For example, if the IFOV of the scanner is 2.5 mrad, the ground size of the pixel in meters is a product of the IFOV (0.0025) and the altitude above ground level in meters.

Important to obtain a strong thermal infrared signal

The inverse-square law states that the intensity of radiation emitted from a point source varies as the inverse square of the distance between source and receiver.

Thus, we can obtain a more intense, strong thermal infrared signal if we can get the remote sensor detector as close to the ground as practical.

Compromising resolutions – very important

Most thermal infrared remote sensing investigations try to maintain good radiometric and spatial resolution by:

- selecting a fairly large IFOV such as 2.5 mrad, and
- flying at a relatively low altitude to obtain smaller pixel sizes.

But at lower altitudes, the high spatial resolution may be outweighed by the fact that more flight lines are required to cover the area compared to more efficient coverage at higher altitudes with larger pixels.

A compromise is needed.

APPLICATIONS OF THERMAL REMOTE SENSING

S-3

Sea and Land Surface Temperature Radiometer (SLSTR) covering 9 spectral bands (550–12 000 nm), dual-view scan with swath widths of 1420 km (nadir) and 750 km (backwards)

Main applications in the thermal infrared:

to detect heat stress, which is useful for improving agricultural practices,

to assess the thermal environment in cities which is useful for energy applications and health protection,

to detect and monitor forest fires

Performance	Parameters	SLSTR	AATSR & ATSR-1/2
Swaths	Nadir view	1 400 km	500 km
	Dual view	740 km	500 km
Global coverage revisit time	1 S/C (dual view)	1.9 days	7-14 days
		0.9 days	-
		1 day	7-14 days
		0.5 days	-
SSI at SSP (km)		0.5 km VIS-SWIR 1 km IR-fire	1 km
Spectral channels centre λ (µm)	VIS (not ATSR-1): SWIR: MWIR/TIR: Fire-1/2:	0.555; 0.659; 0.865; 1.375; 1.610; 2.25; 3.74; 10.85; 12; 3.74; 10.85	0.555; 0.659; 0.865; 1.610; 3.74; 10.85; 12; -
Radiometric resolution	VIS (a=0.5%): SWIR (a=0.5%):	SNR > 20 SNR > 20	SNR > 20 SNR > 20
	MWIR (T=270K): TIR (T=270K): Fire-1 (<500 K): Fire-2 (<400 K):	NeΔT < 80 mK NeΔT < 50 mK NeΔT < 1K NeΔT < 0.5 K	NeΔT < 80 mK NeΔT < 50 mK
Radiometric accuracy	VIS-SWIR: (a=2-100%)	< 2% (BOL) < 5% (EOL)	< 5%
	MWIR-TIR (265-310K): Fire (<500k):	< 0.1 k (goal) < 3 K	< 0.1 K
Life time (in orbit)		7.5 years	AATSR: 5 year design, operative since 2002; ATSR-2: 3 year design, operating from 1995 to 2008; ATSR-1: 3 year design, operating from 1991 to 2000

Climate Dynamics

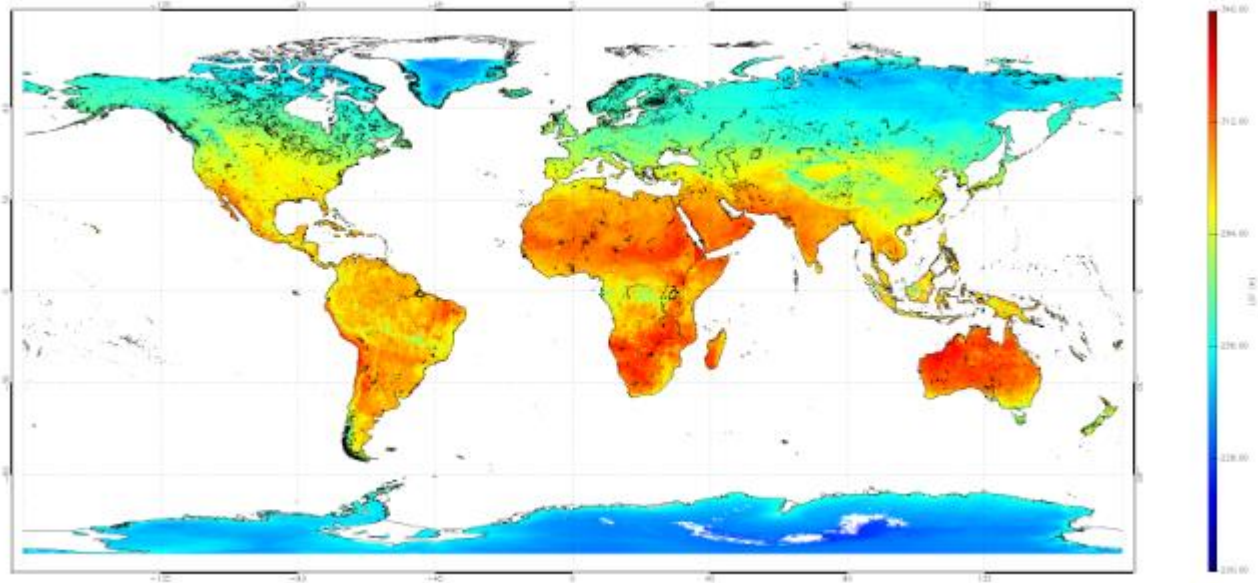

Information from Sentinel-3A's radiometer, which measures radiation emitted from Earth's surface, reveal how the temperature of Earth's land changes between July and November 2016. Measurements are in Kelvin.

Forest fire detection

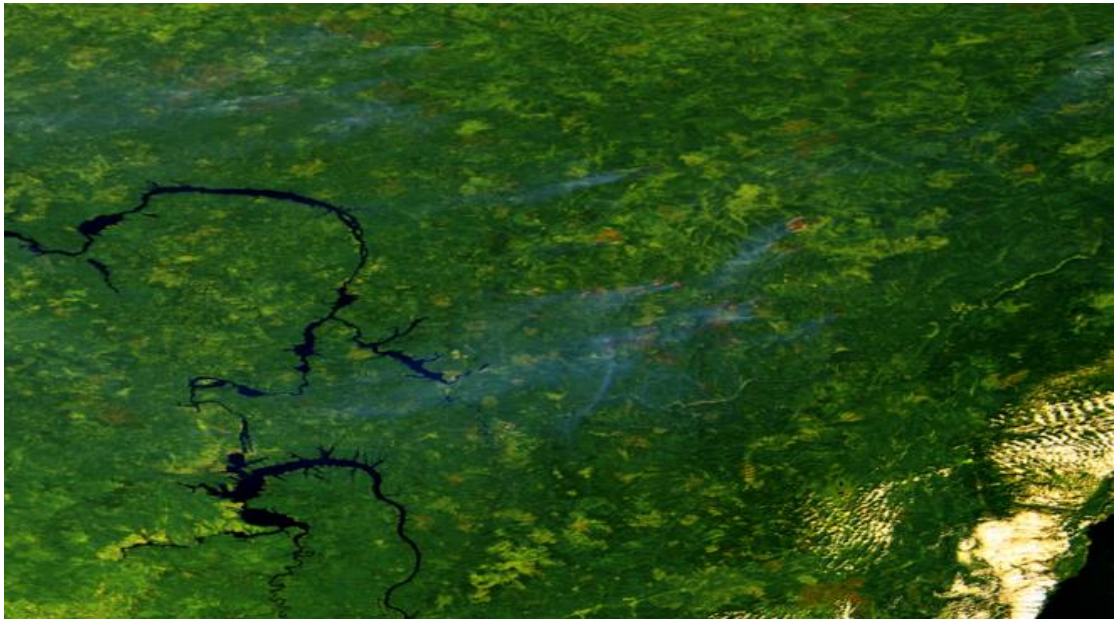

Wildfires break out in the boreal forests of eastern Russia most summers, but 2016 has been particularly bad, with numerous blazes since July. This image, which was taken by the Copernicus Sentinel-3A satellite on 14 September, shows a string of fires northwest of Lake Baikal in Siberia

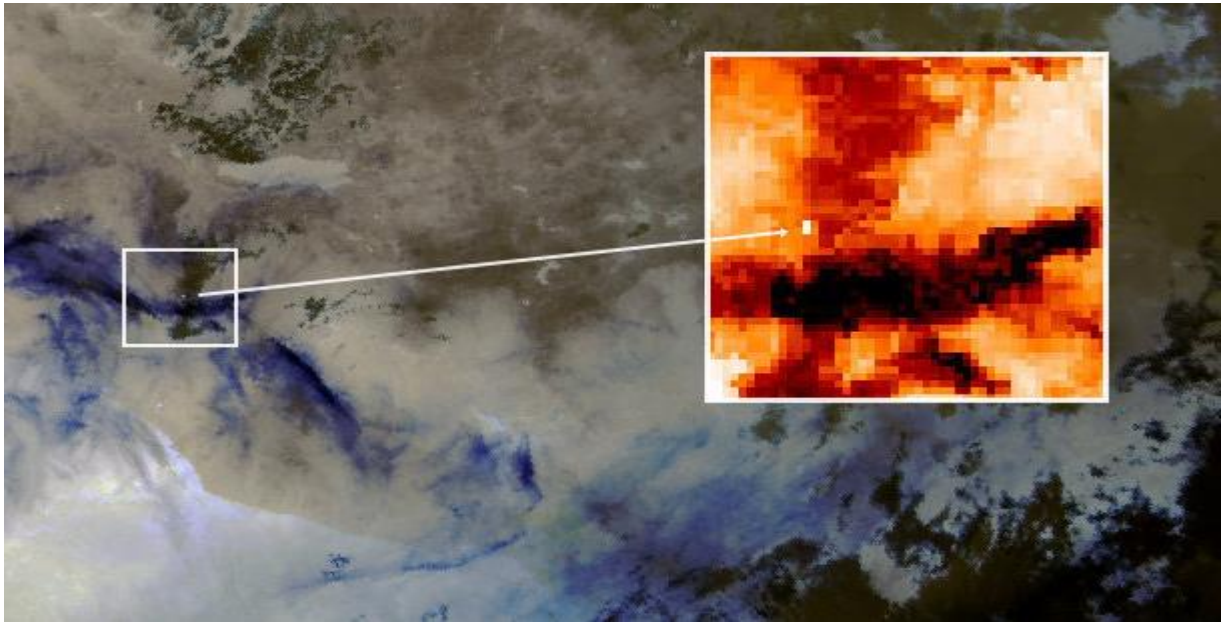

This image from Sentinel-3A's Sea and Land Surface Temperature Radiometer was acquired on 11 October 2016, after Mexico's Colima eruption

Land surface temperature dynamics

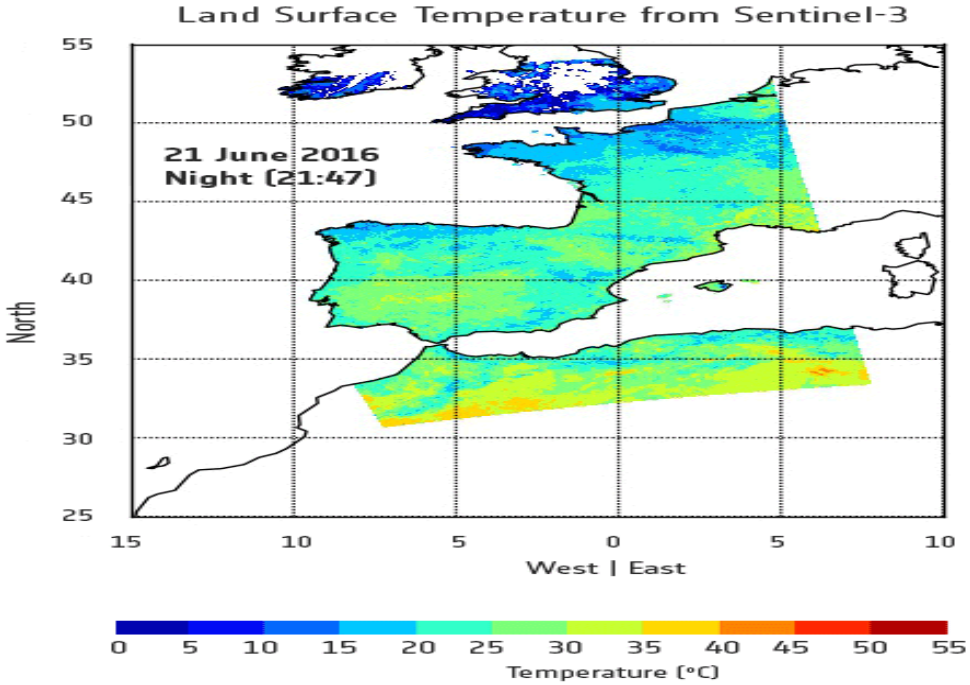


Hungarian
Space Office
SZENT ISTVÁN
UNIVERSITY
esa
FOREST FIRES

Remote sensing and forest fires

Remote sensing can contribute to the three phases of fire management:

Pre-fire: Fuel conditions and amount

Active fires: detection and fire properties **(THERMAL)**

Post-fire: burned area, severity and emissions

Active fires: the thermal signal is discrete**,** especially when using instruments that do not saturate at low temperature. Confusion may be introduced due to signals from oil refineries and volcanic eruptions.

One of the limitations of active fires is that they represent a snapshot, an instantaneous overview at the time of satellite overpass, because the thermal signal is very short-lived.

Wien's law

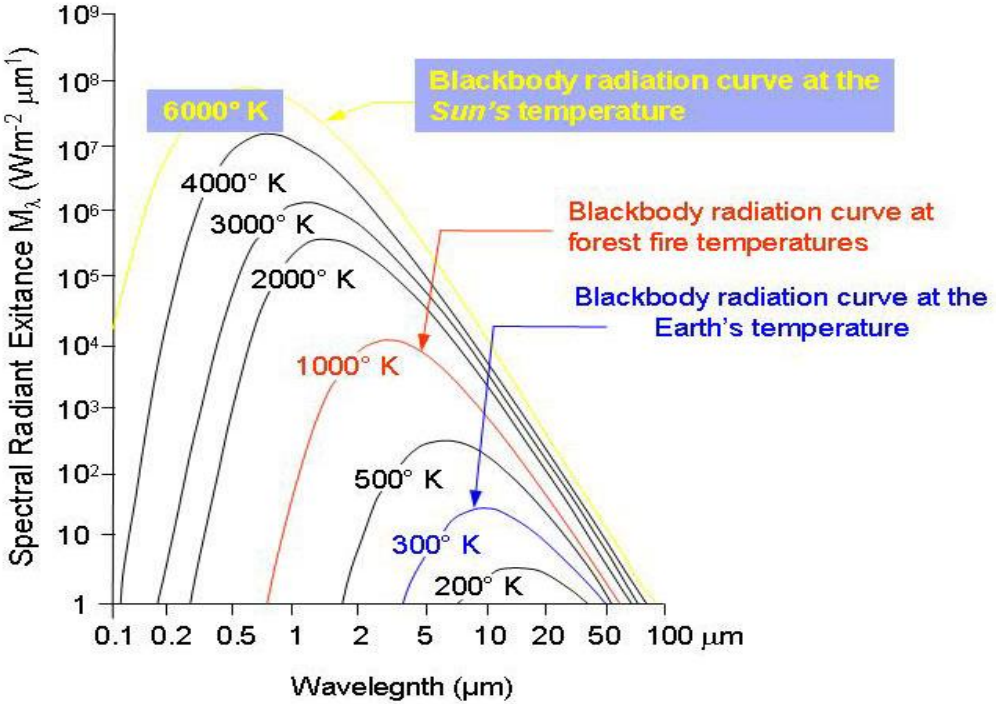
Blackbody radiation curve at the Sun's temperature
6000° K
4000° K
3000° K
2000° K
1000° K
500° K
300° K
200° K
Blackbody radiation curve at forest fire temperatures
Blackbody radiation curve at the Earth's temperature
Spectral Radiant Exitance M_λ (Wm^{-2} μm^{-1})
10^9
10^8
10^7
10^6
10^5
10^4
10^3
10^2
10
1
0.1 0.2 0.5 1 2 5 10 20 50 100 μm
Wavelegnth (μm)

- A fire at 500K will be sensed, as it grows
- first by 3.9μm(at ~100m)
- second by 2.2μm (250m)
- third by 10.8μm (400m)
- An RGB=(3.9;2.2;10.8) might be a good indicator for severity of a fire.
- For a hotter fire (1000K), typically gas flares, channels in the solar domain react faster than 3.9μm

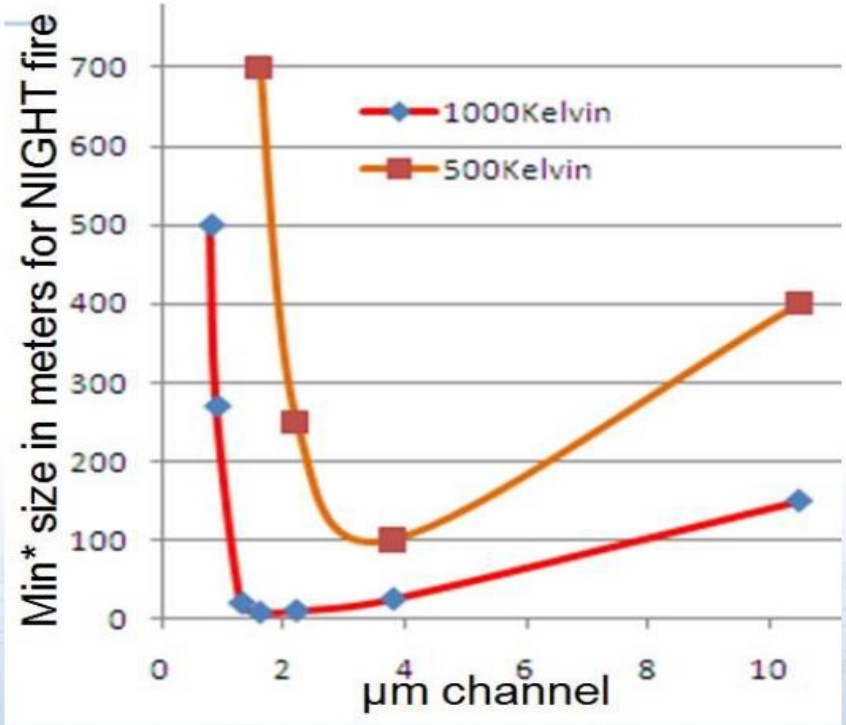

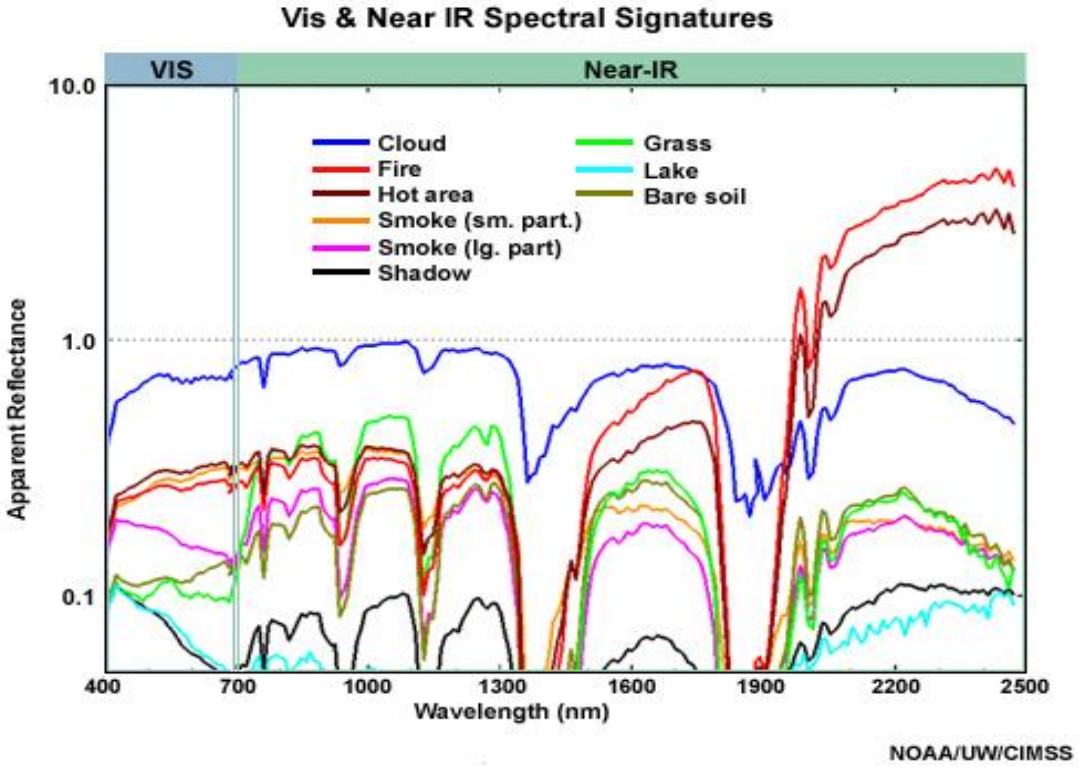
Vis & Near IR Spectral Signatures
VIS
Near-IR
10.0
1.0
0.1
Apparent Reflectance
Cloud
Fire
Hot area
Smoke (sm. part.)
Smoke (lg. part)
Shadow
Grass
Lake
Bare soil
400
700
1000
1300
1600
1900
2200
2500
Wavelength (nm)
NOAA/UW/CIMSS

Comparing window channels in the thermal infrared

Near infrared (1.6 μm)	More adequate for smoke detection than 3.9 μm Small fires not visible No CO2 absorption (higher fire temperature) High sub pixel sensitivity
Middle infrared (3.9 μm)	High temperature sensitivity - major sub pixel effects (hot spots are easily detected) Negligible absorption by atmospheric humidity Close to a CO2 absorption band, 4-7 Kelvin signal reduction Brightness is temperature of the CO2 layer above the fire
Thermal infrared (10.8 μm)	1-2 Kelvin absorption by atmospheric humidity No signal reduction by CO2 Lower temperature sensitivity (small subpixel effects) No risk of sensor blinding by fires Low values compared with 3.9 μm due to semi transparent cloud or smoke

Sub pixel response

Assume a fire occupying an entire pixel on a clear dry night (no clouds and no solar radiation). In this case, the temperature across the pixel would be approximately uniform and we should expect the same radiance temperature at the 3.9 μm and 10.8 μm bands! In this case, it would not be possible to identify a fire pixel by comparing the two bands.

For a pixel partly covered by a fire, the radiance at 3.9 μm is larger than at 10.8 μm due to the stronger response at 3.9 μm to the warmer portion (fire) inside the pixel.

Using the temperature difference IR3.9-IR10.8 as a proxy for fire probability - the larger the difference, the higher the probability.

Fires in Greece

This image of Greece was captured by the Moderate Resolution Imaging Spectroradiometer (MODIS) on NASA's Terra satellite on August 26, and places where MODIS detected actively burning fires are outlined in red. A line of fires stretches along the western coast of Greece's Peloponnesus Peninsula. To the northeast, a large fire is casting a plume of smoke over Athens

LAND SURFACE TEMPERATURE - HEAT STRESS + LONG TERM TRENDS

Slides 54-69,
Remote Sensing and Image Processing Unit,
University of Athens (K. Argyrouli)

Road map to estimate Land Surface Temperature

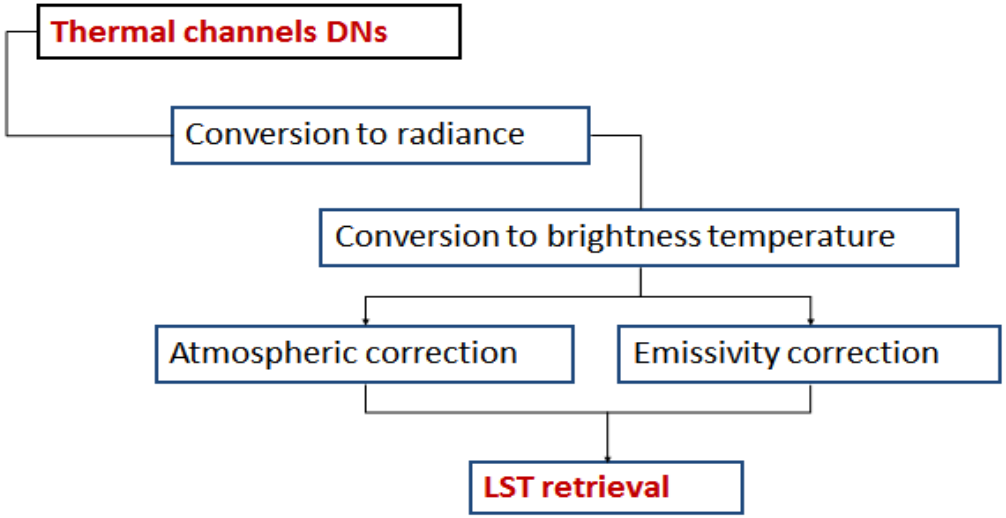

Overall LST accuracy: ±2 Kelvin

Support of Urban Resilience and Climate Adaptability Plans
(Land surface emissivity (left) and Land Surface Temperature (right)

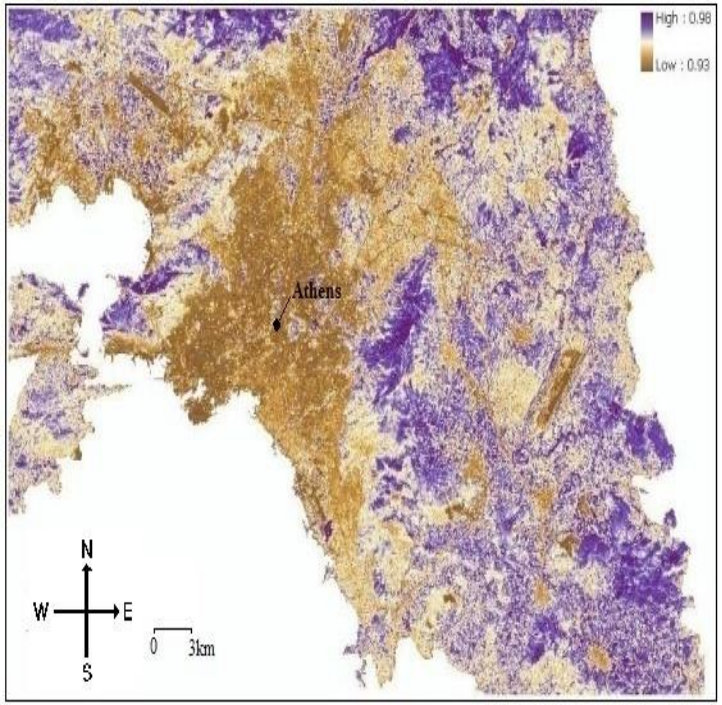

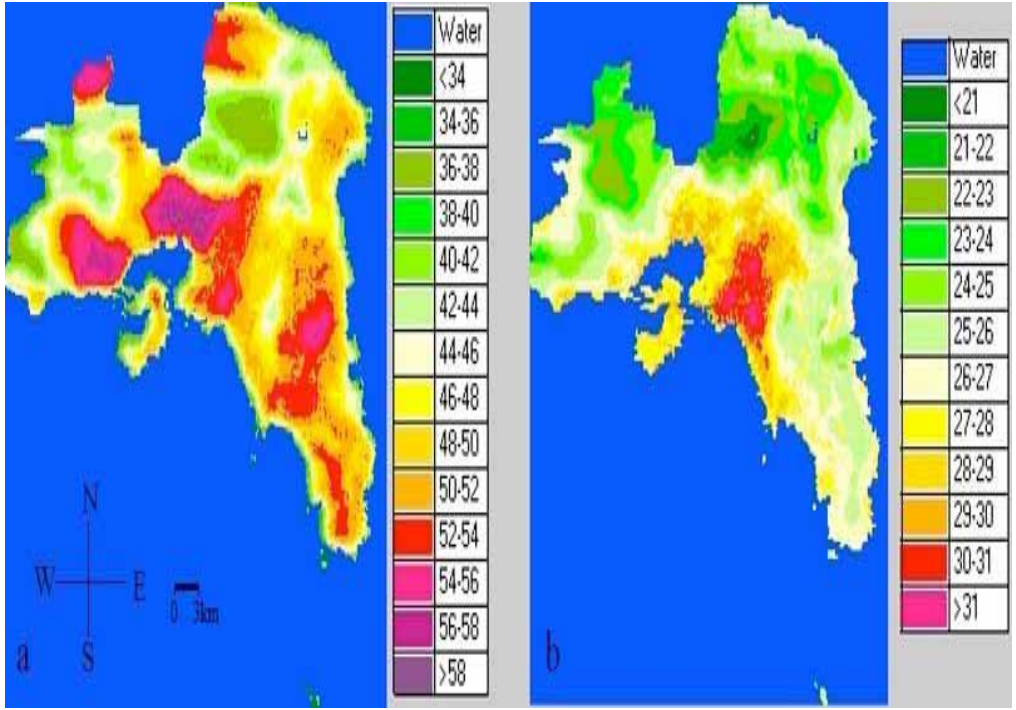

Day

Night

Long term trends in LST

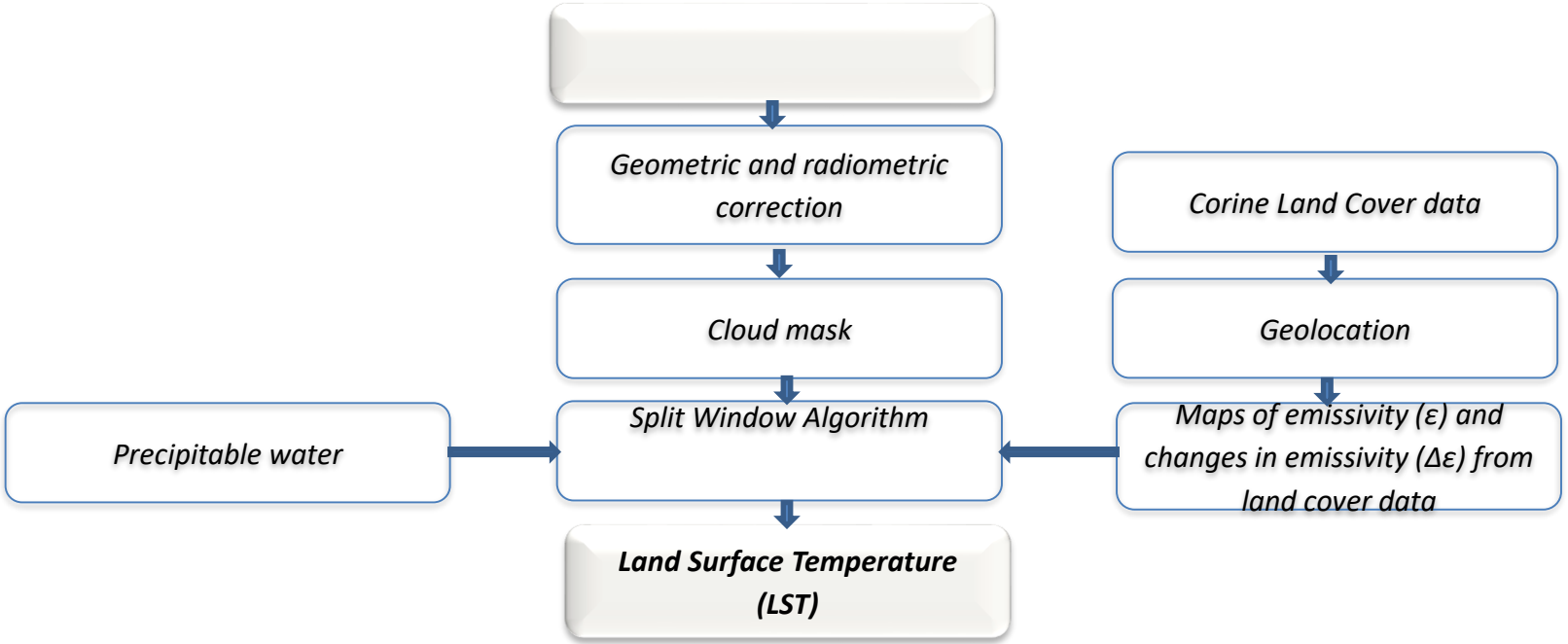

$$LSTtrend(\%) = \frac{lST(2015) - LST(1995)}{LST(1995)} 100$$

Cloud mask

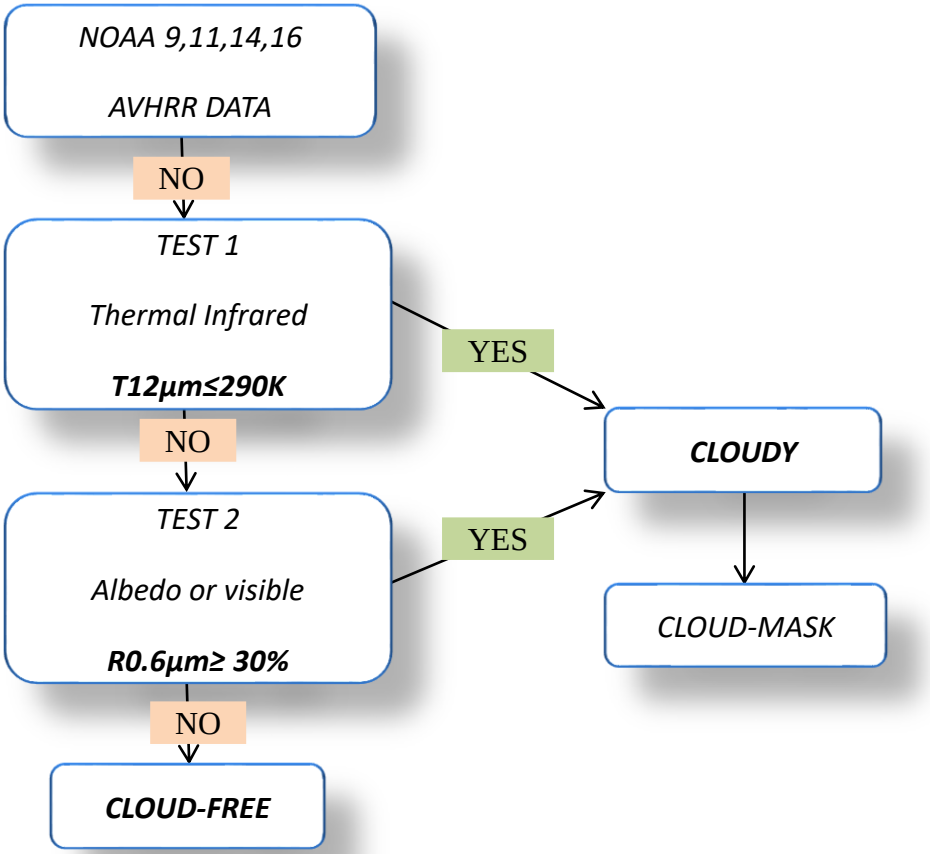

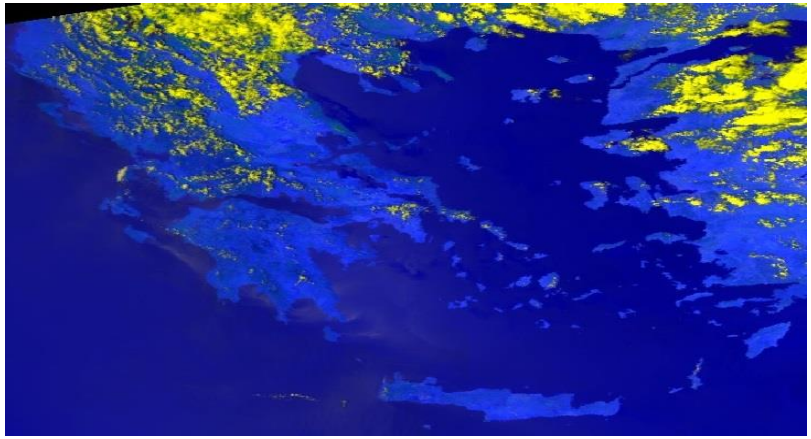

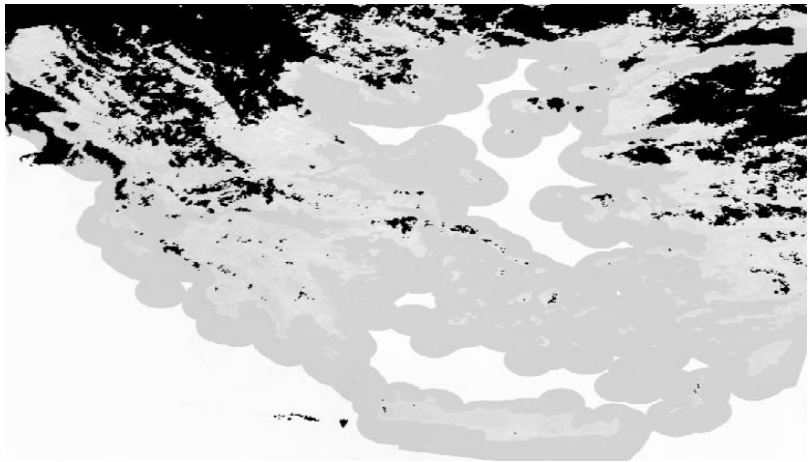

NOAA-19 (2014-12 UTC)

CORINE LAND COVER

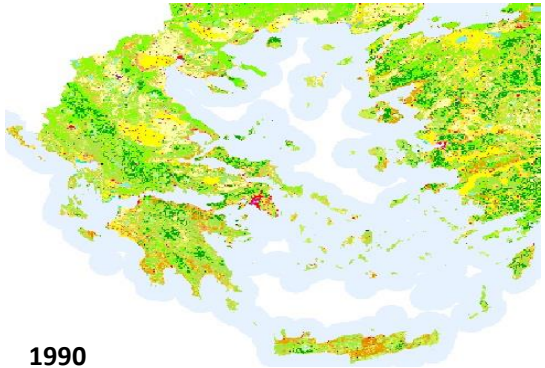

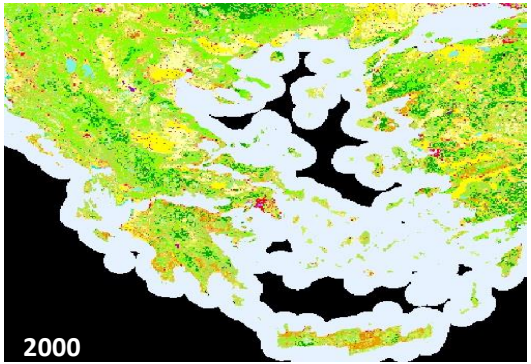

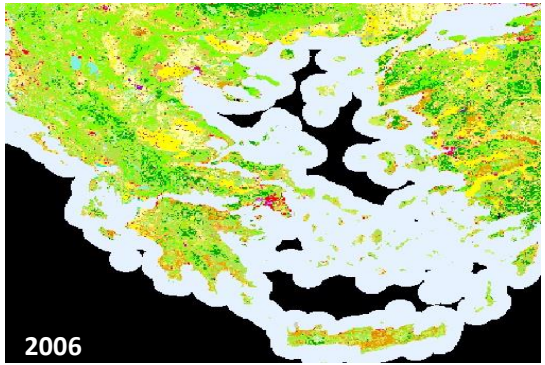

Corine Land Cover

Extraction of ε and change of ε, depending on land cover

Area	Δε	E
Urban	-0.007	0.97
Semi-urban	-0.003	0.98
Rural	0	0.989

SPLIT WINDOW ALGORITHM

$$T = 0.51 + T_4 + (T_4 + T_5) + 0.58(T_4 - T_5)^2 + a(1 - \varepsilon) - b\Delta\varepsilon$$

T_4 = brightness temperature channel 4
T_5 = brightness temperature channel 5
ε = mean spectral emissivity for channels 4 and 5

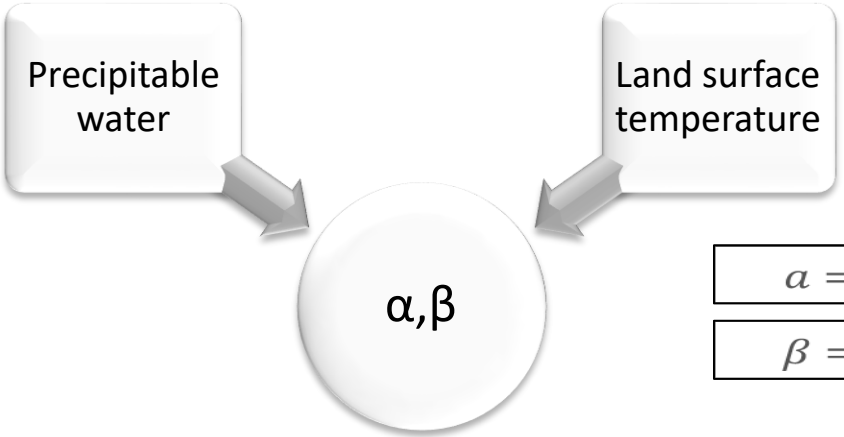

12:00 UTC	PW (gr/cm²)
July	1.669

$$a = (0.190 \cdot PW - 0.103)T_4 - 67 \cdot PW + 107$$

$$\beta = (0.100 \cdot PW - 1.118)T_4 - 68 \cdot PW + 163$$

Center of Athens

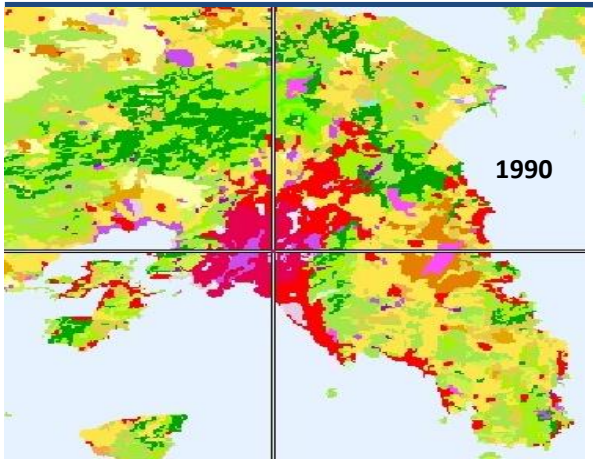

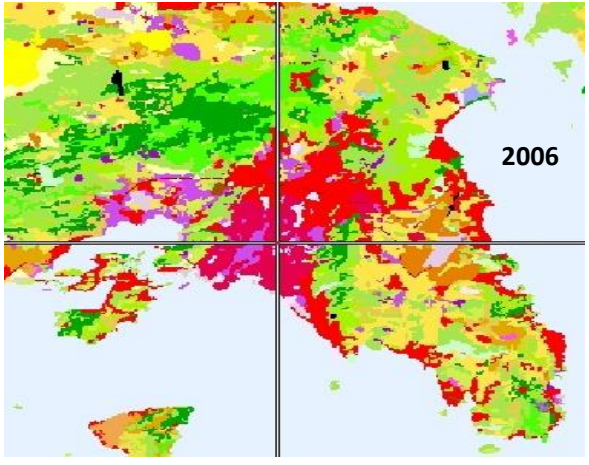

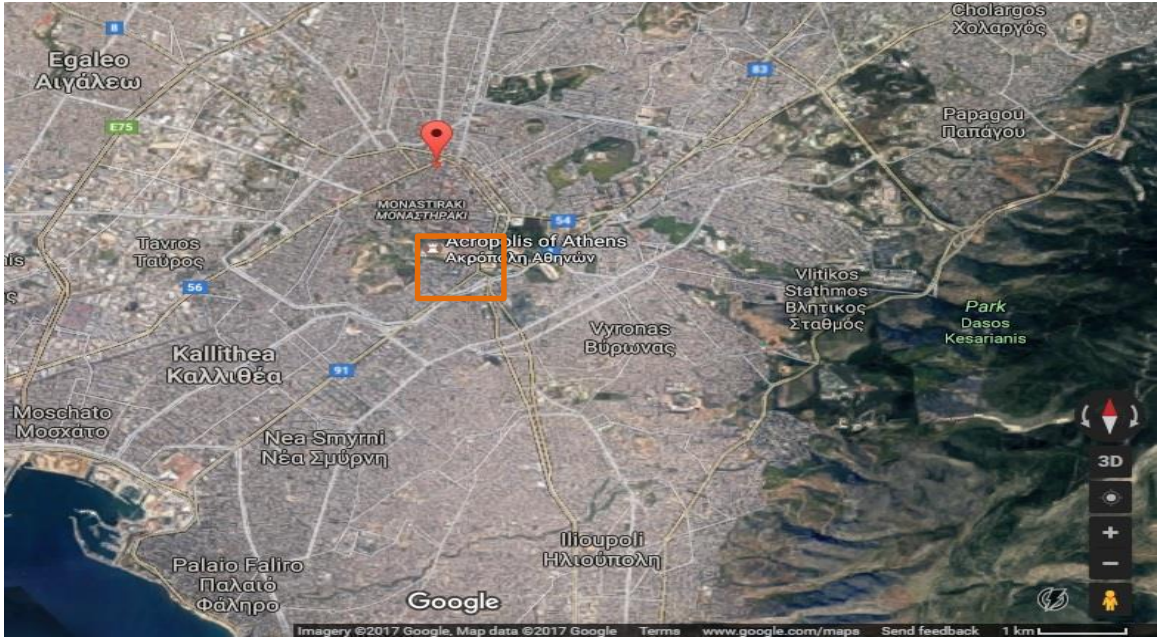

Center of Athens

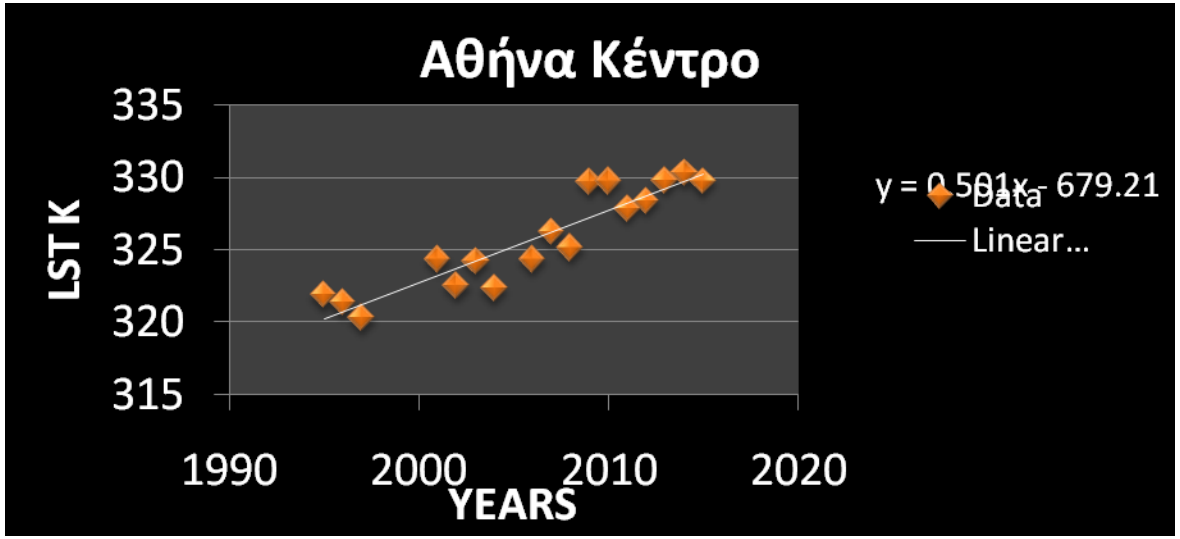

Mean value	325.763 K
Trend	3.1 %
Increase	10 K

Landscape change – from natural to built (airport of Athens)

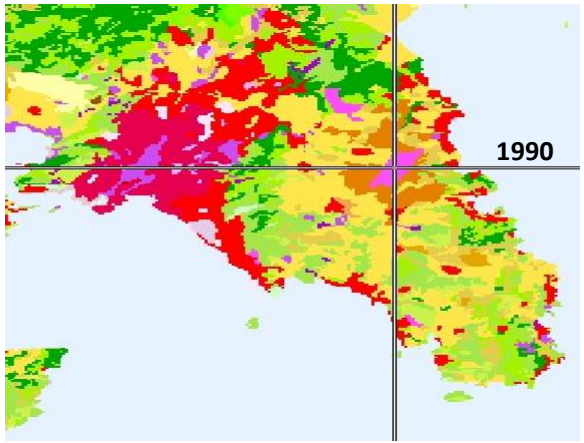

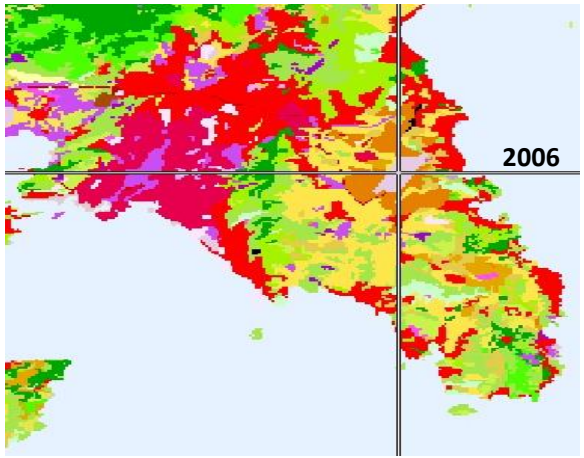

- Airport since 2001. Previously agricultural/rural areas

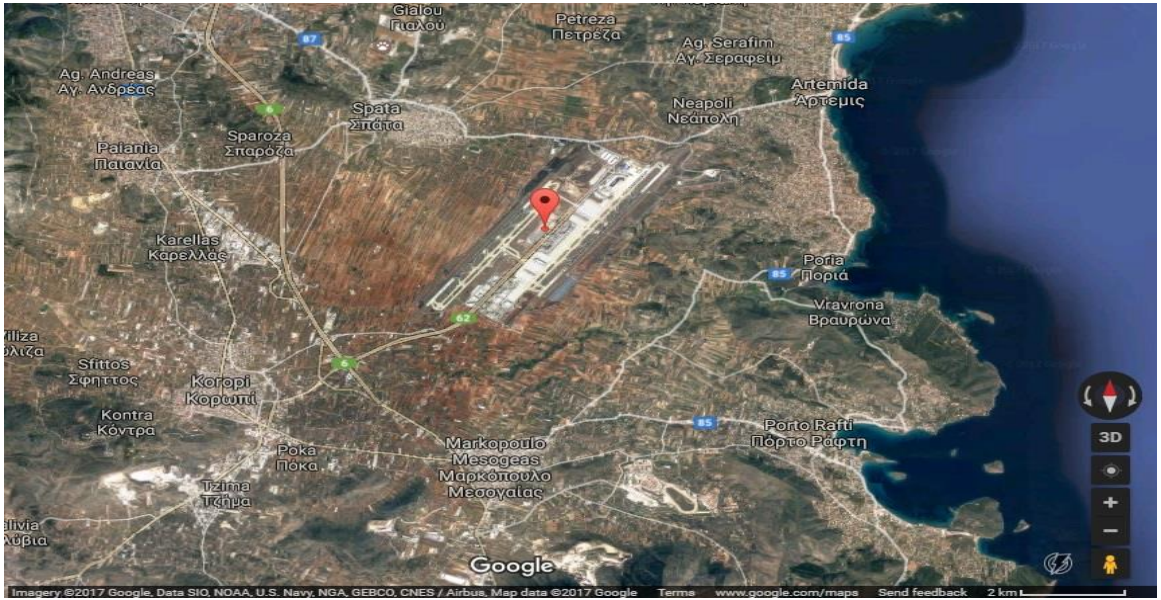

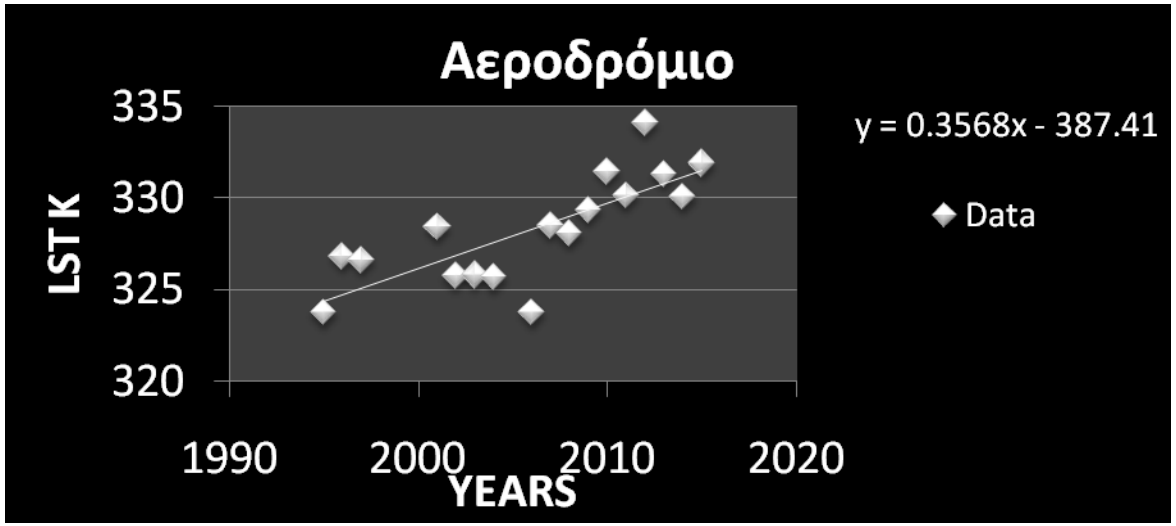

Mean value	**328.320 K**
Trend	**2.1 %**
Increase	**6.8 K**

Industrial areas

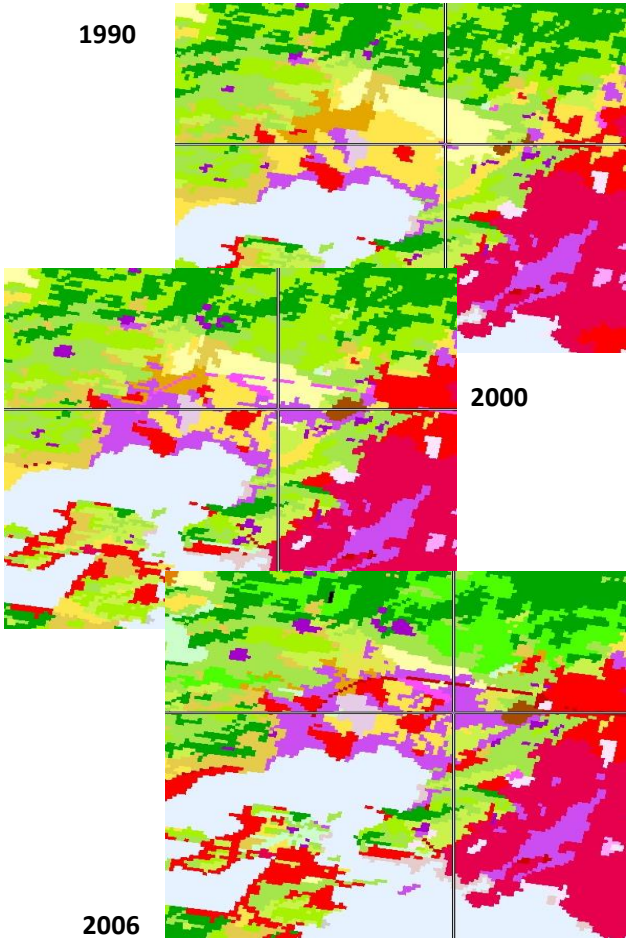

- Industrial area since 1990

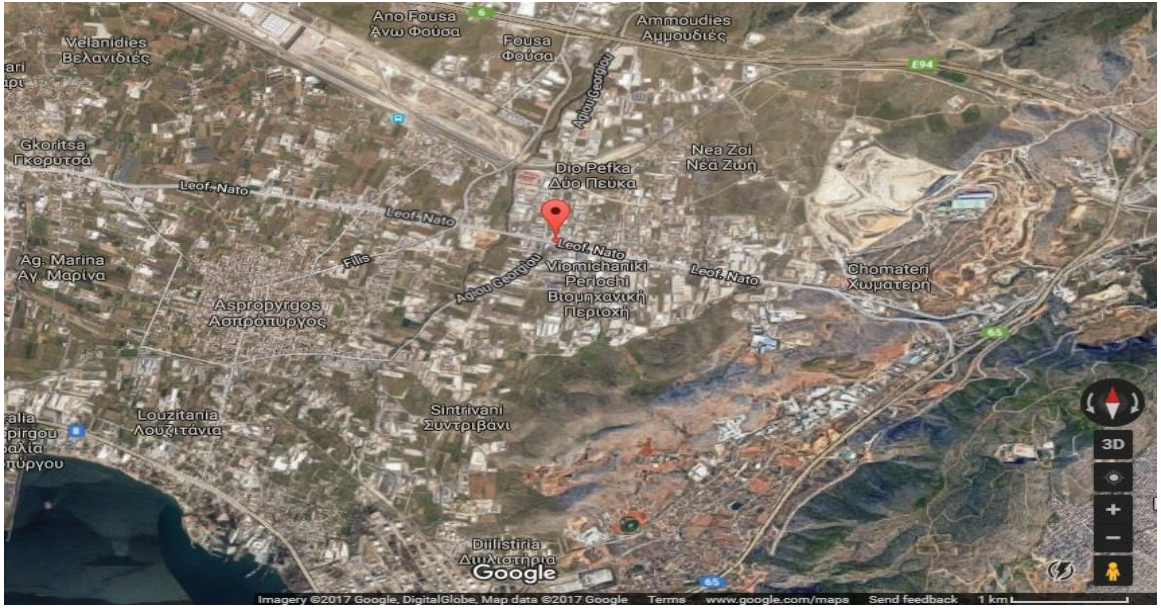

Industrial area

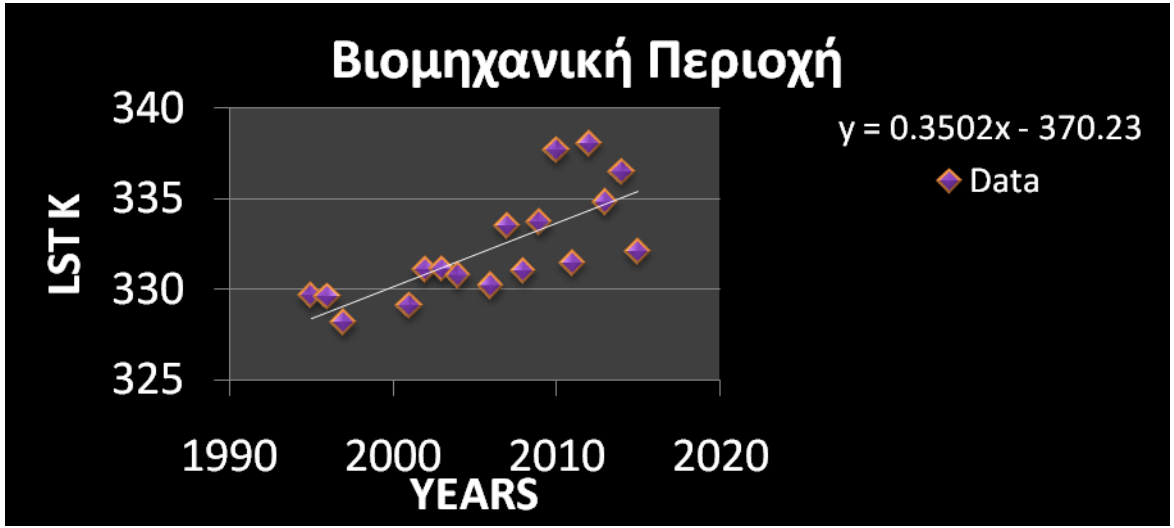

Mean value	332.268 K
Trend	2.1 %
Increase	7 K

Mountainous area

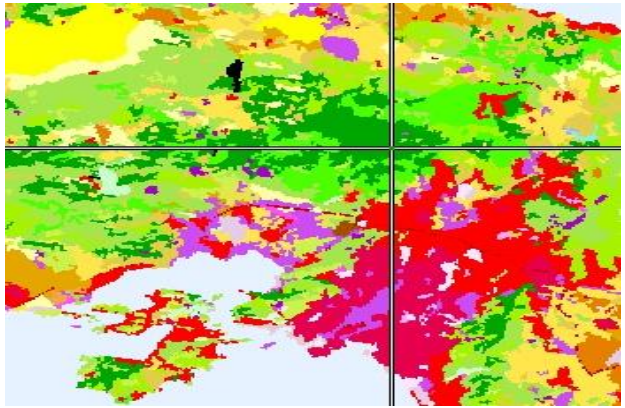

2006

- Forested from 1990 to 2007
- Devastating fire – July 2007
- Reforestation > 2007

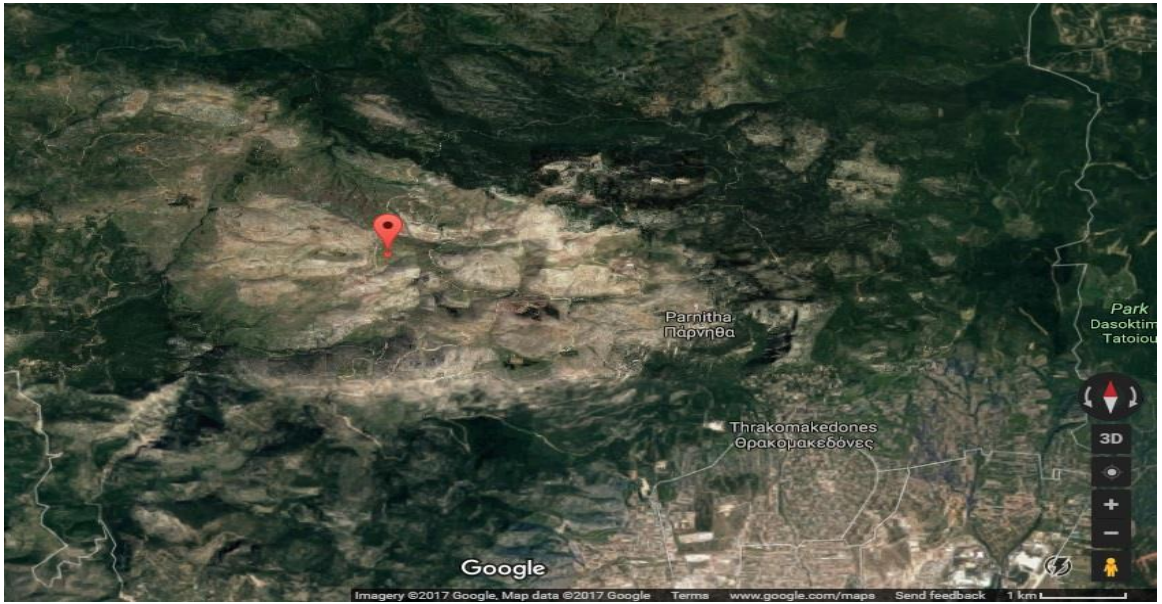

Mountainous area

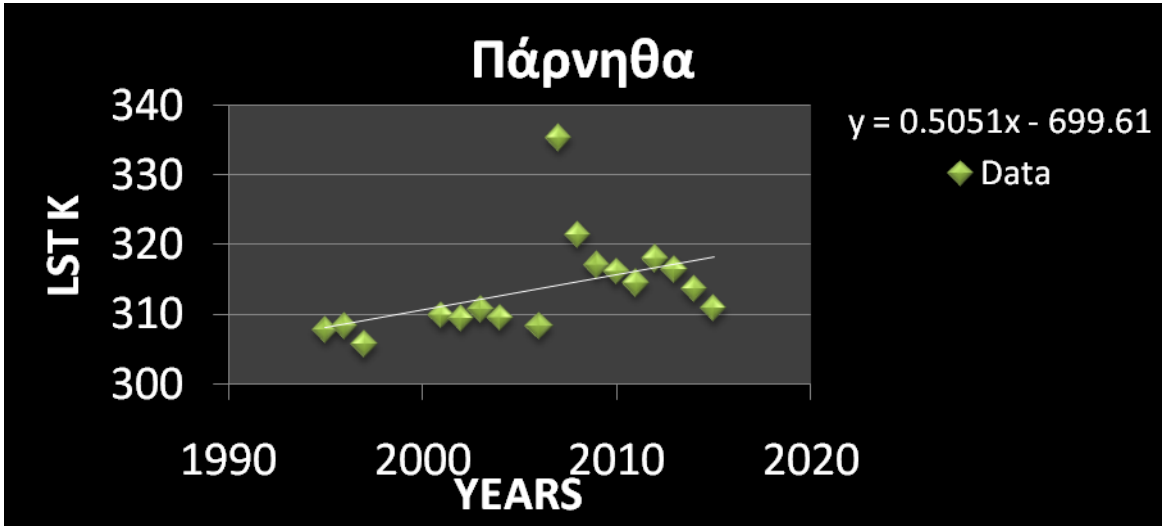

Mean value	313.694 K
Trend	3.2 %
Increase	10 K

Nature reserve (Natura 2000 network)

2006

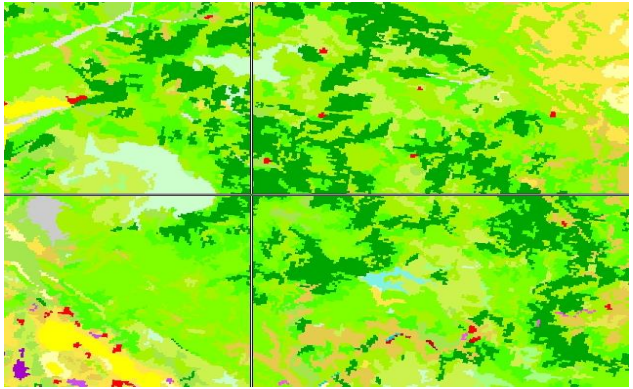

- Forested area throughout the study period

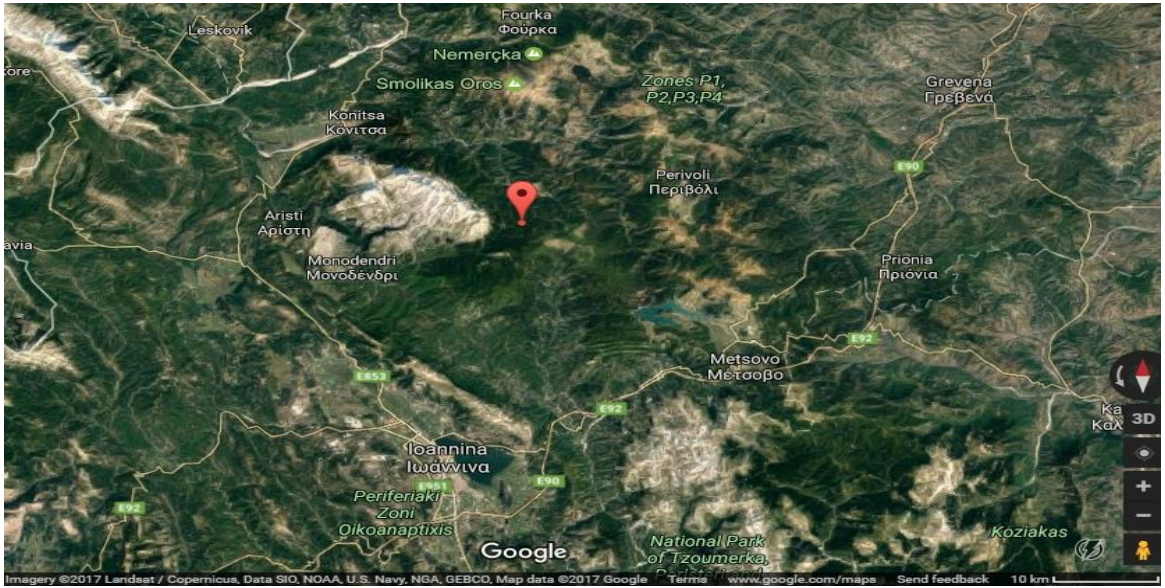

Nature reserve

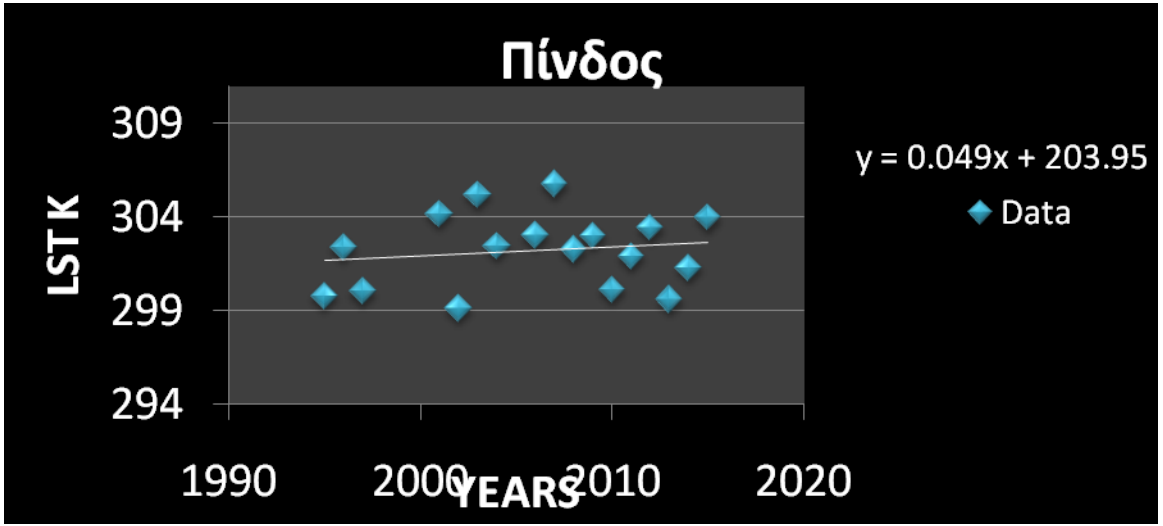

Mean value	302.224 K
Trend	0.3 %
Increase	0.9 K

Agricultural area with water shortage issues

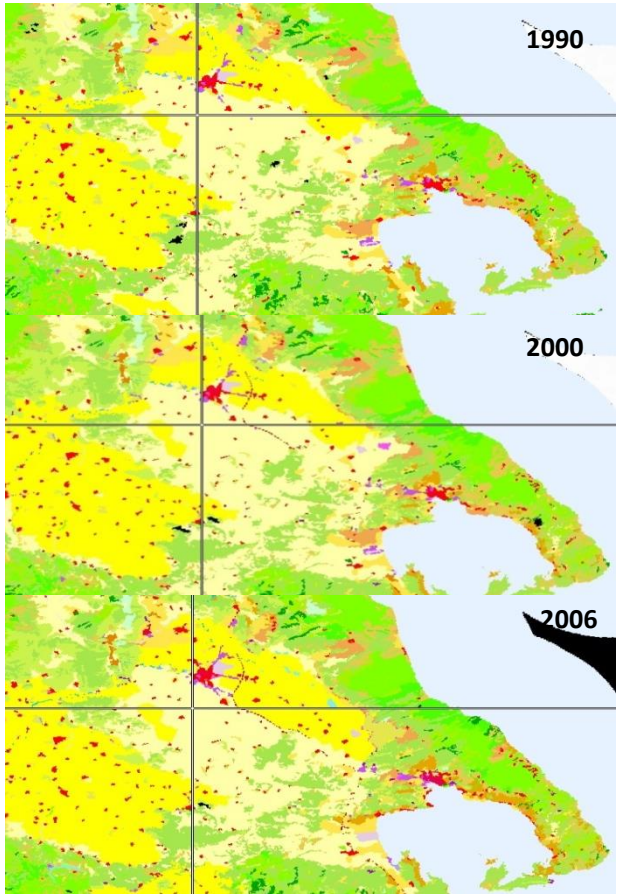

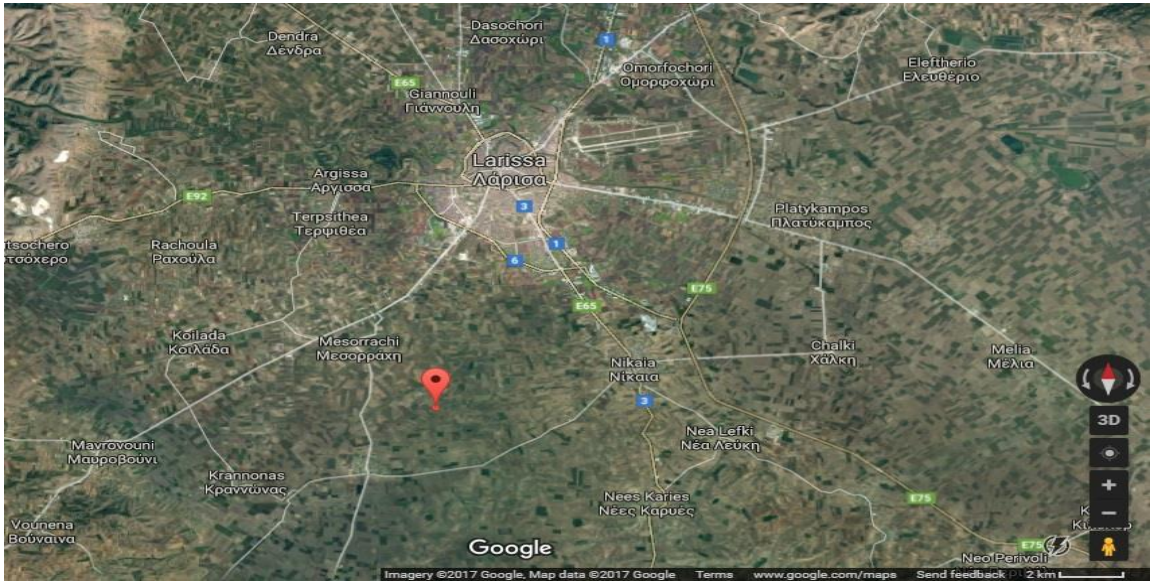

Agricultural area with water shortage issues

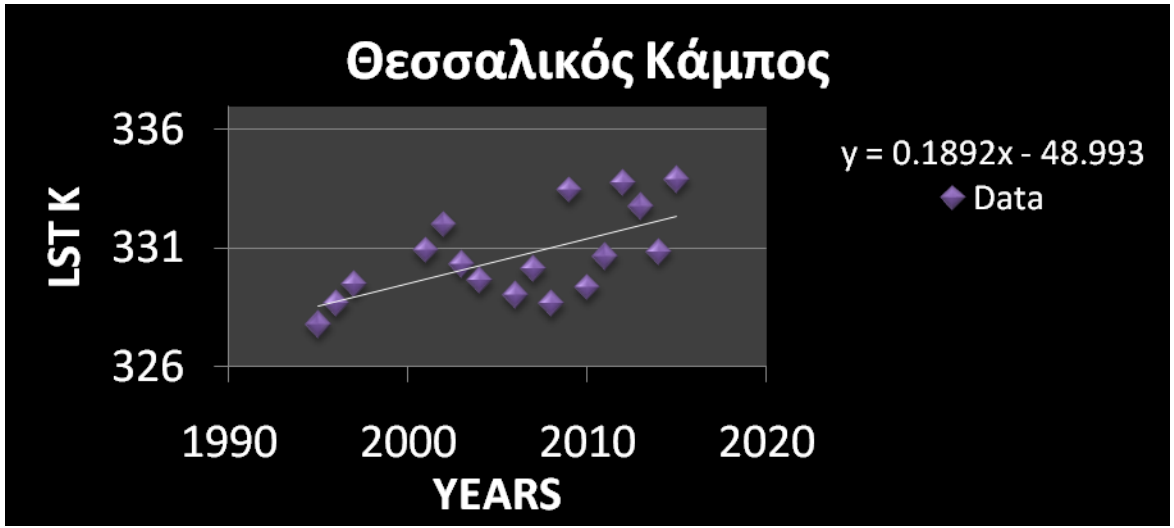

Mean value	330.651 K
Trend	1.1 %
Increase	3.5 K


Hungarian
Space Office
SZENT ISTVÁN
UNIVERSITY
esa
URBAN FLUXES

Estimating anthropogenic heat flux

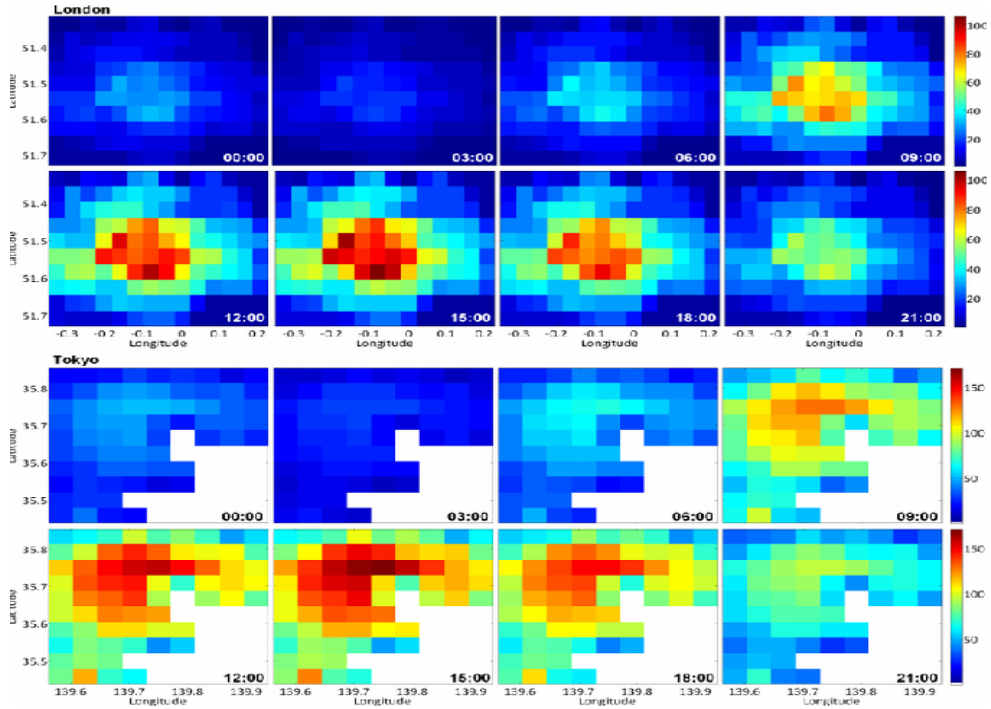

Source: Allen, L, Lindberg, F & Grimmond, S 2011, 'Global to city scale model for anthropogenic heat flux: Model and variability' *INTERNATIONAL JOURNAL OF CLIMATOLOGY*.

ASSESSING THE THERMAL ENVIRONMENT IN URBAN AREAS WITH THE USE OF LAND COVER AND LAND SURFACE EMISSIVITY DATA OF VARYING SPATIAL RESOLUTIONS

CLASSIFICATION LANDSAT – 8 IMAGE

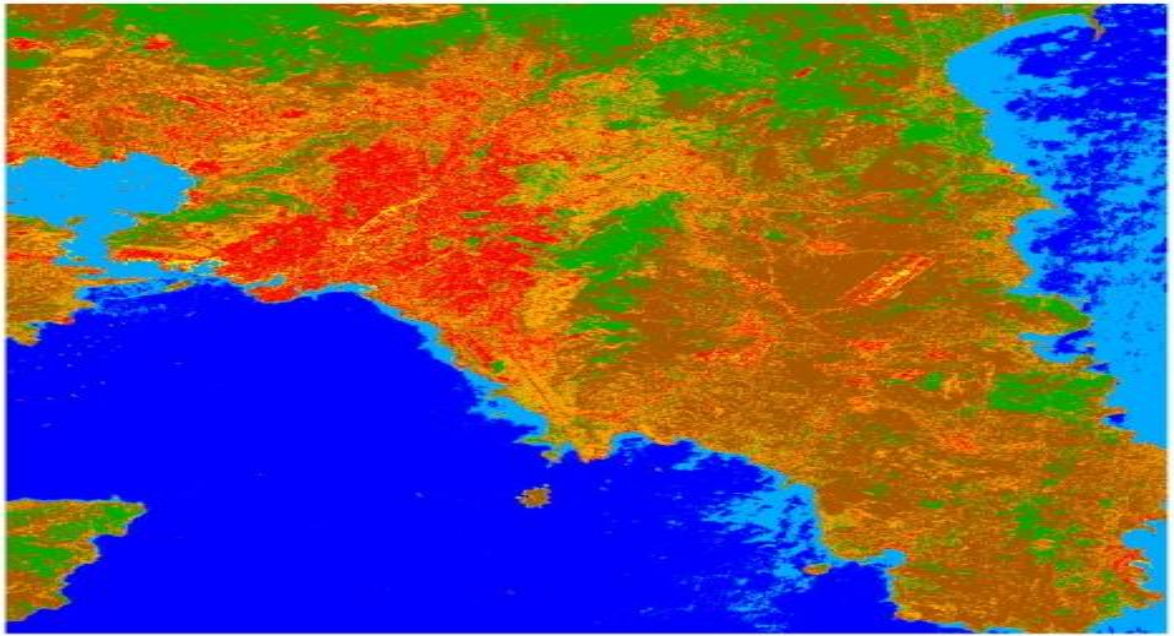

Source for Slides 71-79, Remote Sensing and Image Processing Unit ,Univ. of Athens, 2017 (G. Giannakogiorgos)

CLASSIFICATION SENTINEL -2 IMAGE

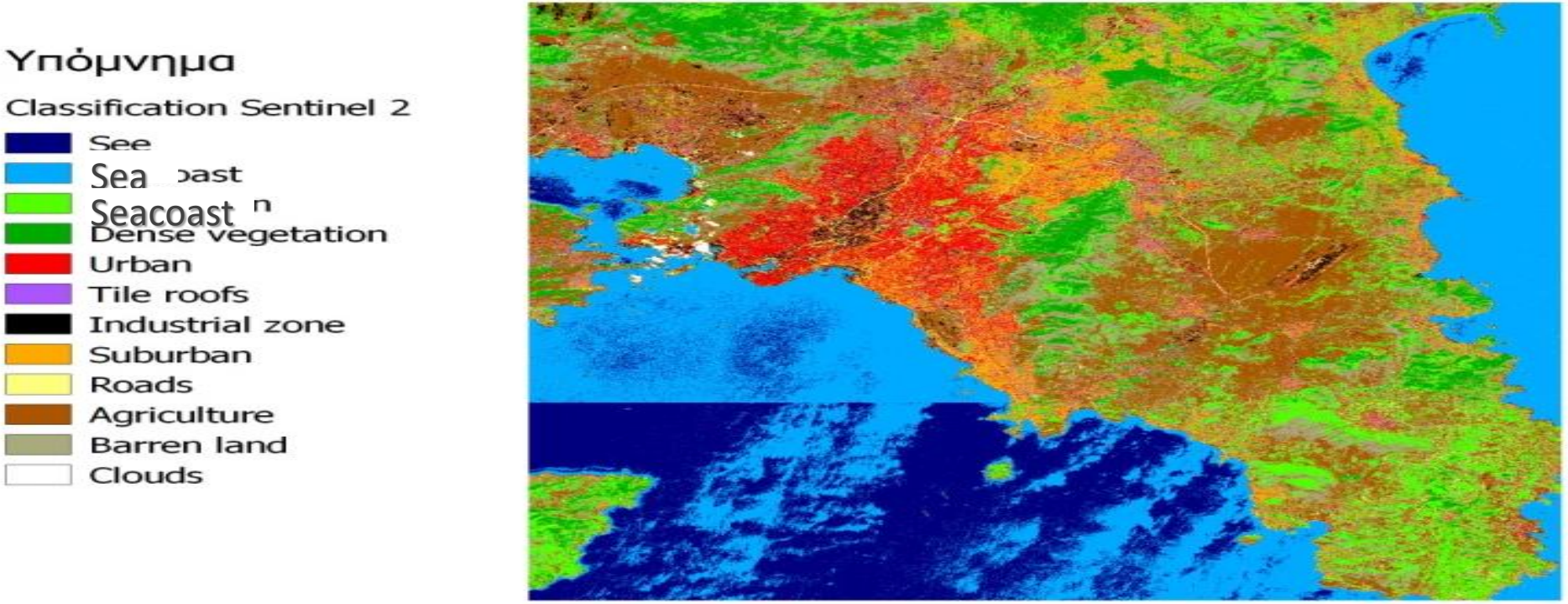

ACCURACY ASSESSMENT

Accuracy = (sum of elements of principal diagonal / total number)

Landsat - 8 68.73%

Sentinel -2 73.82%

NON HOMOGENEOUS AREAS

Εικόνα Landsat 8

Υπόμνημα

Classification non homogeneous Landsat 8

- Urban
- Kallimarmaro
- Roads
- Columns of the Temple of Olympian Zeus
- Vegetation

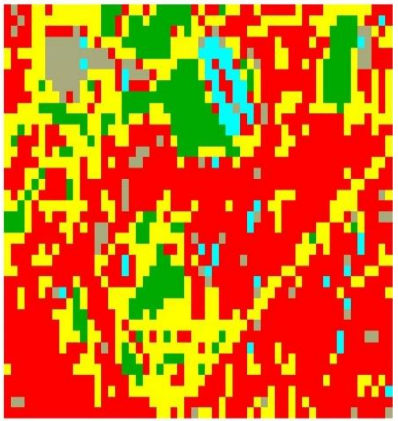

Εικόνα Sentinel 2

Υπόμνημα

Classification non homogeneous Sentinel 2

- Urban
- Kallimarmaro
- Roads
- Columns of the Temple of Olympian Zeus
- Vegetation

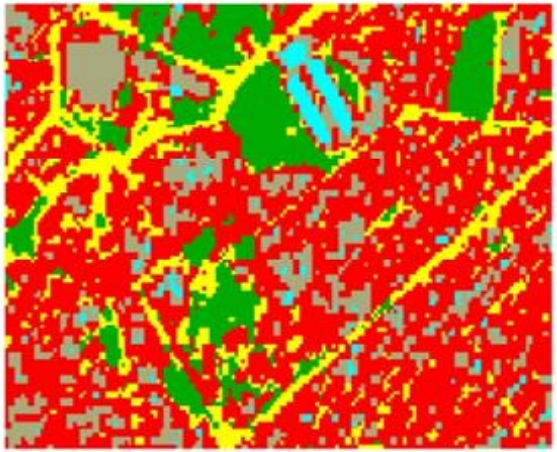

ASSESSMENT OF EMISSIVITY ON THE BASIS OF LANDSAT -8 (left) and SENTINEL -2 (right) LAND COVER CLASSIFICATION

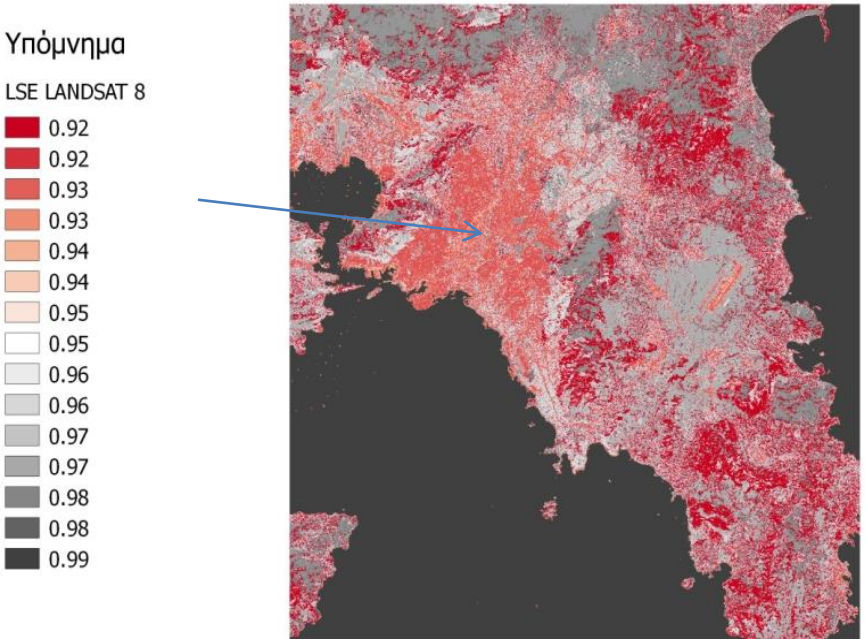

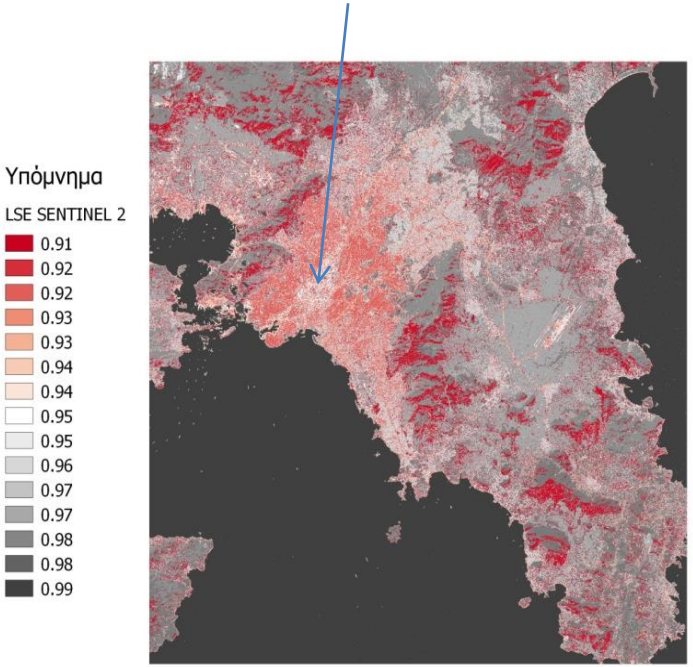

LSE: NON HOMOGENEOUS AREAS

Εικόνα Landsat 8

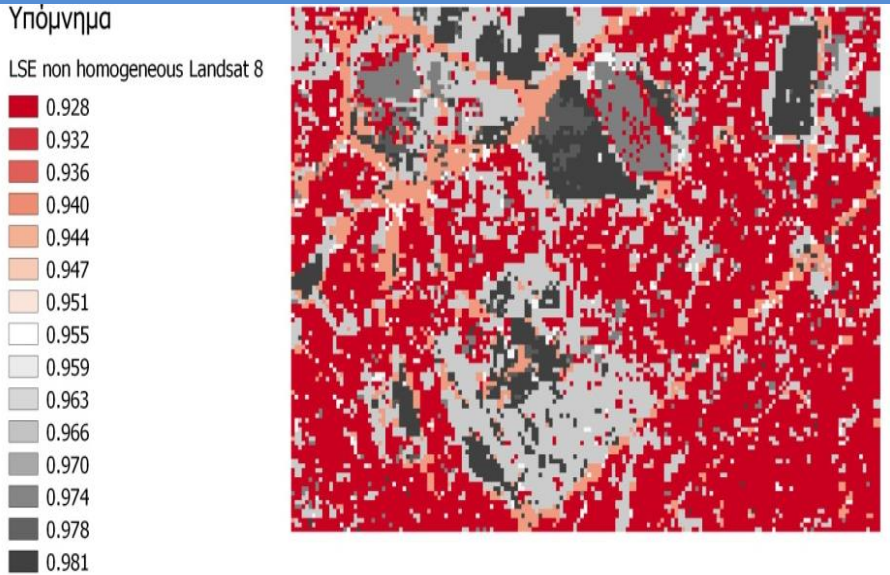

Εικόνα Sentinel 2

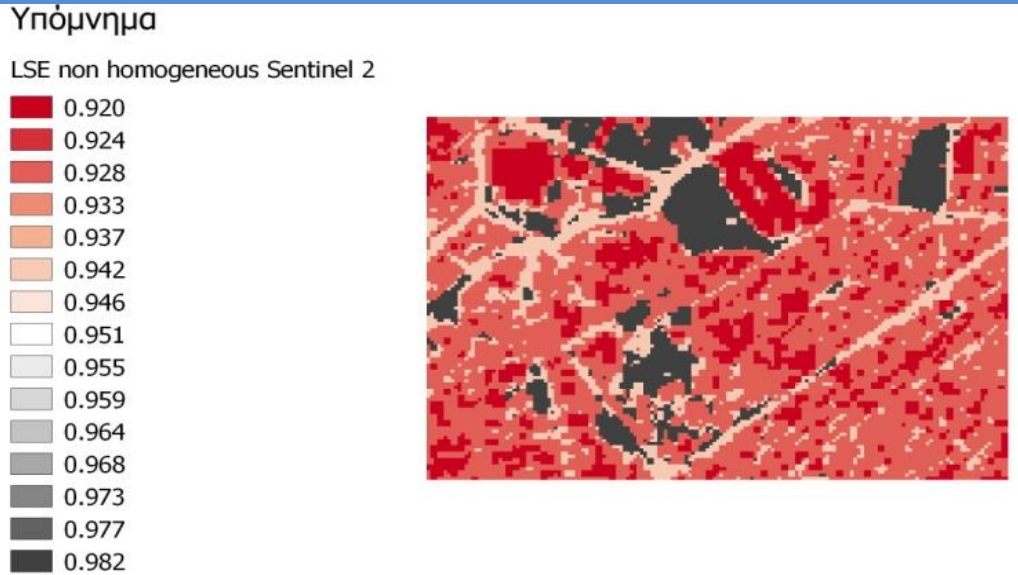

LST as estimated with the use of land cover deduced from LANDSAT – 8 (left) AND SENTINEL – 2 (right)

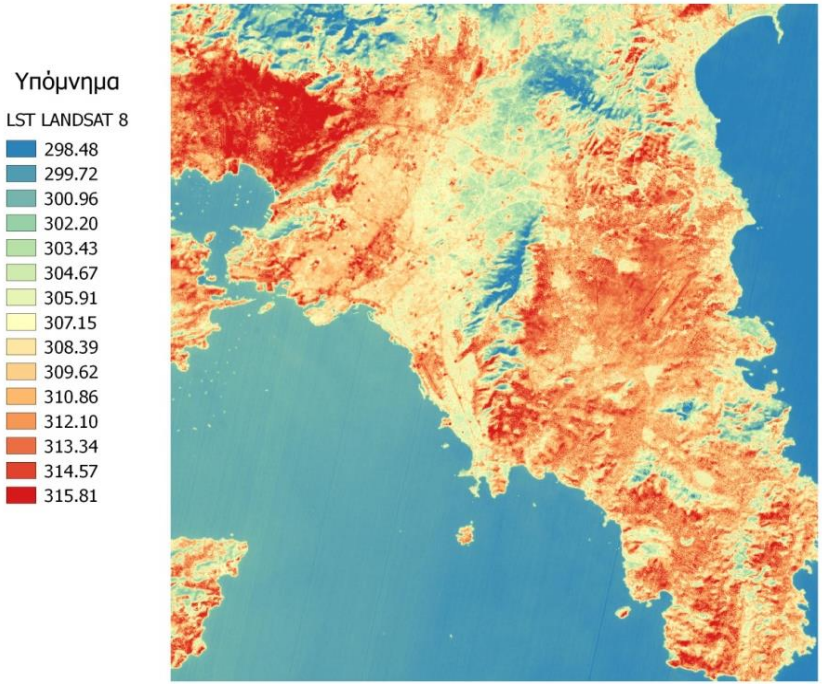

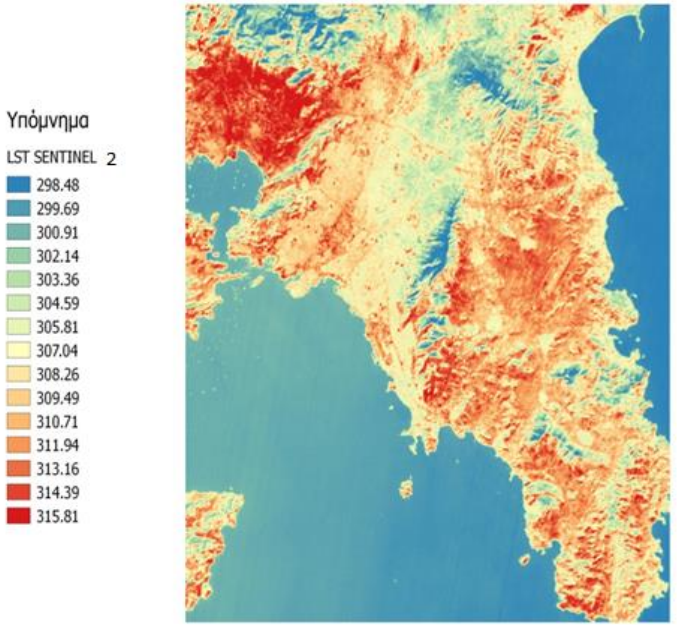

LST: NON HOMOGENEOUS AREAS

with land cover from Landsat 8

LST non homogeneous Landsat 8

- 303.84
- 304.42
- 305.00
- 305.59
- 306.17
- 306.75
- 307.33
- 307.92
- 308.50
- 309.08
- 309.67
- 310.25
- 310.83
- 311.41
- 312.00

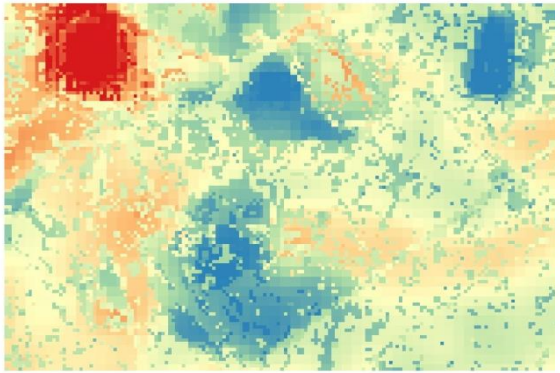

with land cover from Sentinel 2

LST non homogeneous Sentinel 2

- 303.73
- 304.39
- 305.06
- 305.73
- 306.40
- 307.06
- 307.73
- 308.40
- 309.07
- 309.73
- 310.40
- 311.07
- 311.74
- 312.40
- 313.07

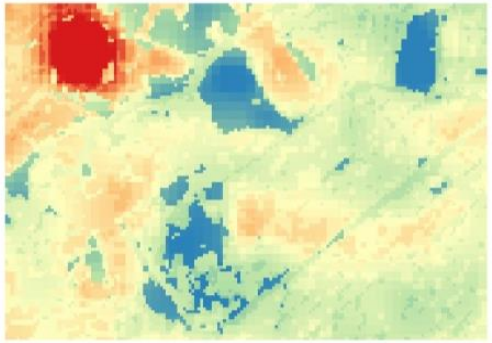

COMPARISON OF AIR TEMPERATURE AS EXTRACTED FROM LST

(Ta = 1.2104Ts - 17.676)

(Stathopoulou and Cartalis, 2005)

STATIONS	$T_{air\ data}$(C)	$T_{air\ Sentinel}$(C)	$T_{airdata}$-T_{Sent}C)	$T_{air\ Landsat}$(C)	$T_{airdata}$-$T_{Landsat}$(C)
1	25,3	24,6	0,7	26,1	-0,8
2	24,4	24,6	-0,2	24,7	-0,3
3	25	24,5	0,5	24,4	0,6
4	25,7	25,2	0,5	24,6	1,1
5	25	24,6	0,4	26,5	-1,5
6	22,7	21,2	1,5	19,9	2,8
7	24,4	24,7	-0,3	25,4	-1
8	24,3	24,4	-0,1	25,4	-1,1
9	24,9	23,9	1	23,9	1
10	25,2	24,8	0,4	24,5	0,7
11	23,8	23,5	0,3	25,2	-1,4
12	24,2	25,1	-0,9	25,6	-1,4

TIR imaging has an advantage in this regard in that even thick smoke is transparent at these wavelengths allowing imaging of hotspots through smoke. This can be a useful property in monitoring active fires and searching for spot fires.

Another advantage of TIR (over shorter wavelength IR) imaging is that the dynamic range of the scene in the presence of fire is limited in the TIR, making it easier to image both the fire and background without saturating the sensor.